Turnantenna Documentation

Release 1

Musuuu

Aug 20, 2018

Contents:

Author Marco Musumeci

The Turnantenna project is a Ninux IoT experiment. The original idea came from the mind of Salvatore Moretti, whom developed the very first prototype with Edoardo Putti and started this project. I met Salvatore and Edoardo during the weekly Ninux meet-ups in Florence (IT) and I started working of his idea applying my mechanical knowledge. Few months later Leonardo Maccari proposed me to apply to the Google Summer of Code with this project, and I accepted. In the mean time, in 2018, we brought the Turnantenna at the Merge-it@Turin and at the WirelessMeshUp@Berlin, and we'll bring it to the Maker Faire@Rome. I graduated in the middle of the GSOC, and combined the work of my mechanical engineering thesis, with the software development required by Google.

The entire work is described here, and here we'll continuously make updates and link new references. If you'd like to support the project, ask informations, or simply write your opinion, contact us at:

crm.marco@gmail.com

firenze@ml.ninux.org

CHAPTER 1

Introduction

The Global Wireless Mesh Network market is expected to grow from USD 3,45 Billion in 2017 to USD 12,1 Billion in 2026[1], at a Compound Annual Growth Rate (CGAR) of 15%, as a response to the growing adoption of connected devices in industry, army and civil applications.

WMNs use directional and omni-directional antennas. The first ones are capable of reaching very far distances, and are the-best fit solution for networks that serve vast environments; however, since directional antennas can't change their pointing direction, the topology results to be static and stiff, and a local failure can have repercussions at the macro level.

When the network needs to change dynamically, (e.g. in case of upgrades, problem-fixings, optimizations) directional antennas have to be rotated either manually or with an automated system. The solution provided by this work is a light, low power consuming self-rotating remotely controlled system, called Turnantenna.

The design process of the Turnantenna follows a practical approach: theoretical solutions that comes from physical analysis are systematically tested in practice with the realization of a prototype. The Turnantenna is primarily thought to be used by Wireless Community Networks users, whom are inexperienced people. The simplicity of assembly is pursued to give those people the possibility to build the Turnantenna themselves, in order to help networks' growth. The design process is held in close contact with those communities, in particular Ninux, and people whom have a great experience in the field.

The directional antenna is equipped with two stepper motors that allows the rotation around two distinct axis. When the wind blows at the maximum design speed of 37,5 m/s, the entire system consumption is 24W, which is reduced when wind blows in ordinary conditions (<8m/s) and engines could be switch off.

In conclusion, the Turnantenna is a cheap, effective solution for directional antenna problems in WMNs. Industry 4.0 is based on a strong and stable wireless coverage, and the benefits of this system can have a considerable impact on the overall performances for networks that serves big areas.

[1] Research and markets


Google Summer of Code

CHAPTER 2

Wireless Mesh Networks: cases of use

2.1 Introduction to WMNs

A computer network is defined as a telecommunications network, which allows computers to exchange data. In computer networks, networked computing devices exchange data with each other using data links. The connections between nodes are established using either cable media or wireless media[1].

A wireless mesh network, furthermore, is a communications network made up of radio nodes organized in a mesh topology[2]. In this particular configuration, nearby nodes are connected together with a radio link, allowing direct communication between neighbours; couples of nodes far away from each other can get in contact establishing indirect connections using neighbours, neighbours of neighbours and so on.

WMN schemes could be a good alternative to wired ones in many industrial facilities. This because wired communications could be difficult to install, too much costly or not flexible enough to support quick process reconfiguration.

Since 2000s WMN's system was adopted by communities around the world which started to develop an alternative to ISP's networking. Today some of those networks reach tens of thousands of users (e.g. Guifi, Freifunk), which retain the full control and ownership of the infrastructure, and benefit from exclusive independent services.

2.1.1 Business Applications

WMNs should be considered as a good choice in different scenarios. Industry 4.0 and "smart factories" are based on real time control and interconnection between machines; a flexible and reliable network is becoming a key weapon for the industries. A one-size-fits-all network system doesn't exist: physical wiring and radio transmission can be used, even together, to match the best cost-benefit balance.

Wireless networks can significantly enhance the efficiency, productivity, safety, security and scalability in small and large production plants, especially where other systems lacks (e.g. wiring, cellular coverage, ecc.), providing cost effective communications for process control sensors.

Examples of WMNs are given by:

[1] Wikipedia, "Computer network", 2018
[2] Wikipedia, "Wireless mesh network", 2018

- oil and gas exploration and production plants[3]
- mines
- off-shore systems
- automated meter readings (AMR)
- military forces in field operations
- surveillance
- the 66-satellite Iridium constellation
- wireless internet service providers (WISP)
- digital signage

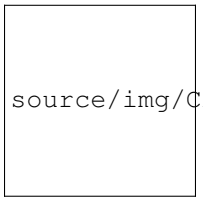

Fig. 1: Figure 1-1 Example of industrial control system, TropOS Wireless Communication System ©Copyright 2013 ABB

2.1.2 Pros and Cons

One of the simpler example of the WMN usefulness, because of the large usage of wireless devices, comes from security and video acquisition. Data sources could easily be mobile ones or be installed in insulated locations. In that situation every device, from cameras to antennas, could be a node of the mesh. Every WMN could take advantage from this.

Another absolute upside is redundancy. It works as following: when one node can no longer operate (a), the rest of the nodes can still communicate with each other, directly or through one or more intermediate nodes (b). Doing so, the network's reliability results increasingly higher with increasing number of nodes.

[3] ABB Inc., "Oil and gas exploration and production", 2016, Document ID: 9AKK105713A0311

Fig. 2: Figure 1-2 Example of outdoor surveillance network - Rajant kinetic mesh

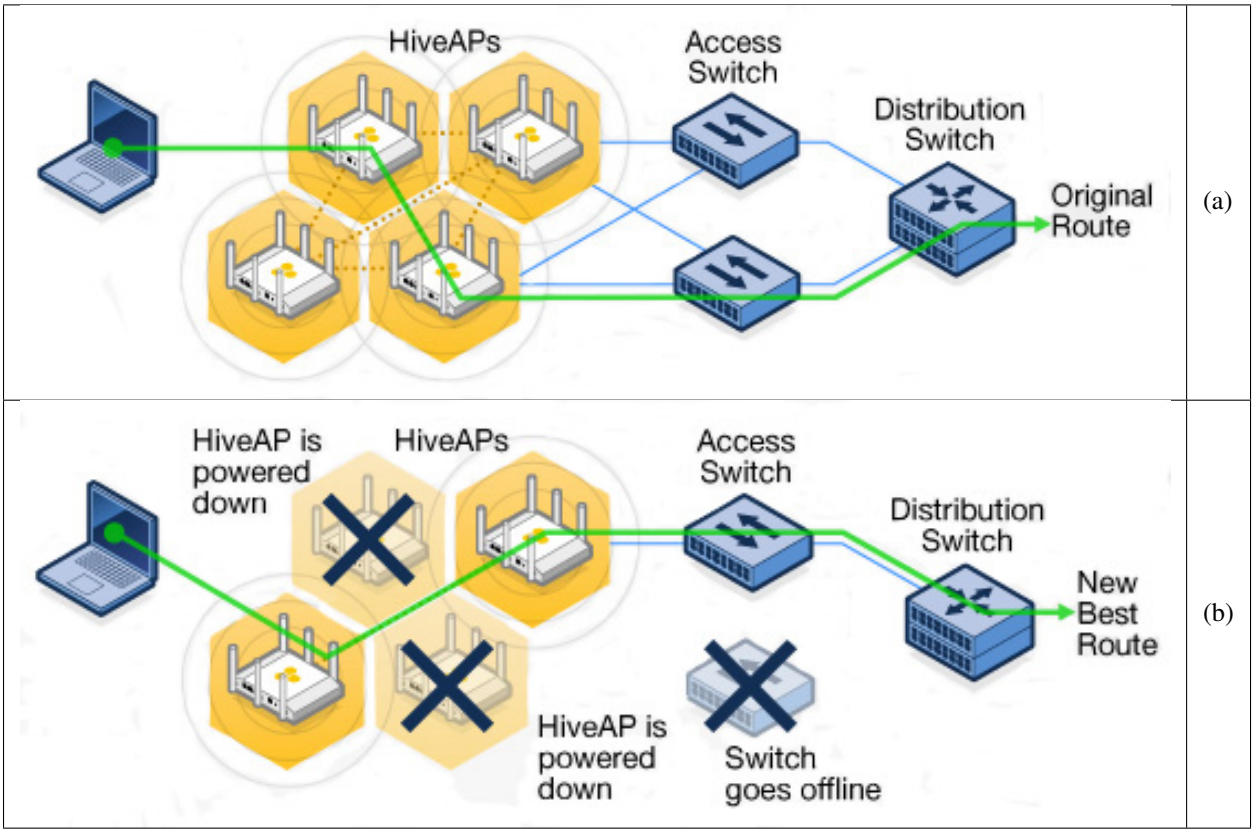

Figure 1-3 Example that clarify redundancy in WMN - aerohiveworks.com

Wireless networks support multiple other applications and user groups concurrently. The same physical infrastructure can be leveraged for applications such as SCADA, emergency shutdown, process control, video analytics, mobility and Wi-Fi access[4].

On the other side, there are some disadvantages while using WMN. The first one regards the network size, in terms of nodes and connections. If the topology is not as dense as required, reliability could be severely compromised, and all the network could be split up in more disconnected islands. Adding more nodes to the network, or applying a hybrid solution with other technologies could solve this problem.

The second major problem concerns performances, more specifically the delay, namely how long it takes for a bit of data to travel across the network from one node or endpoint to another[5].Delay depends on the network protocol, the number of nodes and connections, the topology of the network and the end points of the communication. The reason is that in mesh networks data packets have not a single way to go from point A to point B, this because of the redundancy. The network protocol adopted decides which route is the best, most of times in terms of speed, but in every moment that path could change. The issue lies here, in the fluctuation of the route from point A to point B, that reflects on a contraction or dilatation of the delay. Here again a solution could be provided by a network upgrade.

In conclusion WMN is a brilliant solution for big scale built from scratch networks, and for wide external areas, but a good infrastructure is needed to provide reliability and high performances.

2.1.3 Wireless Community Networks

The most widespread mesh network in the world, capable of addressing the largest number of companies and private citizens, is internet. It is not necessary to spend time explaining why it is so important for our society, but the attention should be focused on its shadow: the digital divide. This phenomenon has to do with that people who don't even know that internet exists, and folks beyond the reach of the fundamental technological breakthroughs. Just to have an idea of the digital divide magnitude, just think that in 2014 the 20% of EU citizens did never use the Internet[6].

The Internet exists thanks to the solid massive infrastructure that provides a physical connection between computers (i.e. copper wires and optical fibre), and a wireless equipment able to establish point-to-point or multi-point links. Through this cluster of links, users can benefit from thousands of services; that transform users in clients, and the infrastructure provider a vendor. The vendor is often a national ISP or another commercial (for-profit) operator. The concentration of customers in small areas and their grouping in buildings, make it a great business for commercial telecom providers; as the population density decreases and the distance to major cities increases or the economic capaciy of customers' decreases, the margin for commercial exploitation decreases or becomes negative[7]. In this scenario is easy to understand why disconnected people are mostly those who live in rural areas.

One of most promising solutions for the digital divide problem are the Wireless Community Networks, which are a particular case of WMNs applied in a community scale. WCNs are bottom-up projects developed by a community of people that builds its own network infrastructure, primarily (but not exclusively) made of wireless links.

This kind of networks, in facts, started in digital divided areas thanks to some of their key features:

- they can be made with very cheap equipment
- they can provide services and digital instruments which fit the community's needs
- if just one node is connected to internet, it can provide internet to the whole network

WCNs now become hundreds, all around the world. New ones where born to provide an alternative to the monopoly of the ISPs (e.g. In New York with NYCmesh.net), or even to fight the data collection of the big companies, or the censorship of some restrictive governments.

[4] ABB Inc., "Top 10 reasons to use ABB Wireless", 2017, Document ID: 4CAE000410 REV 1000 26.7.2017
[5] Wikipedia, "Network delay", 2017
[6] Europa.eu, "EU Digital Divide Infographic", 2014
[7] netCommons, "Report on the Existing CNs and their Organization (v1)", 2016

2.2 Goals of the project

The whole documentation of this project is open source, and its core objective is to improve expandability, maintainability and optimization of WCN in the world. The belief behind this work is that such of networks promote a healthy idea of local cooperation and self-sustenance that works like a catalyst for social and economic innovations.

Since the project is born to help communities, the main objective is keeping the entire system cheap and easy to use. That, inter alia, makes this project fully consistent with productive environments needs.

Before entering into the details, it's useful to preface some definition to better understand following parts of this work.

Antennas are one of key elements for wireless networking, and they could be classified in two macro classes: directional ones and omni-directional ones. Directional antennas could generally provide a long distance communication, but have a slightly concentrated beamwidth; omni-directional antennas, on the other side, provide a 360° coverage angle, but can't reach distances comparable to the other ones.

Omni-directional antennas represent the best solution for indoor installations or, in general, for that situations where an homogeneous spread out network is needed. Those networks are typically made of planar antenna arrays.

Directional antennas are the best solution given for long-range links. This type of antenna is helpful in near LOS (Line-Of-Sight propagation) coverage, such as covering hallways, long corridors, isle structures with spaces in between, etc[8]. The idea of the project is to keep the great advantage offered by the possibility of connecting sparse nodes, without the limitation of having a still and immutable topology. This could be achieved using a remote controlled automatic system capable of changing the antenna orientation.

It is possible to buy some self-rotating directional antenna in the market, but in general they are not suitable for the purposes of this project, since they are heavy weight, difficult to fit on poles, excessive current consuming or too much expensive.

2.2.1 Getting dynamic WMN

Directional antennas are very powerful, as they could establish several kilometres long links; the biggest problem here is the network rigidity. Some nodes could fail, sometimes antennas could be hard to mount correctly or more power could be temporarily needed over a particular area. In those cases the only thing to do is to manually change the topology.

Problems could come from a bad distribution of the data flow. During the network lifetime some links could be overloaded as consequence of periodic events. For example, during the setup of a machine in the production shop, sensors, actuators and video acquisition could be emphasize in order to improve tests reliability. Assume that the network get saturated by this intense data traffic in the zone between the machine and the control centre, like a highway clogged by cars.

In WCN this effect was observed by the Ninux community in Calabria, where the network is all over the Cosenza city. Cosenza is located near a mountain, a strategic point where to install several directional antennas to serve the valley. They did so, and started using that to create new nodes instead of trying to find new paths between urban nodes. As a result, they found themselves with a busy node, slowed down by the heavy traffic.

In these two examples, even if the networks are only locally disturbed, it was possible to observe a considerably degradation of the overall performances. This effect is known as *performance anomaly of 802.11b*[9], and occurs every time a single link uses a lower bit rate than the others of the network. The solution here is to change the mesh topology in order to dilute the traffic through more pats.

Having the possibility to dynamically adapt the mesh every time is needed, is an advantage for the WMN in all the application fields, and helps to reduce the performance anomaly.

[8] Cisco, "Omni Antenna vs. Directional Antenna", 2007, Document ID: 82068

[9] IEEE, M. Heusse, F. Rousseau, G. Berger-Sabbatel, A. Duda, "Performance Anomaly of 802.11b", 2003, DOI: 10.1109/INFCOM.2003.1208921

2.2.2 Benefits for meshers

For all the reasons listed before, a dynamic WMN is capable of reducing the investments in a long-lasting period. The initial higher hardware cost is balanced by an easier and faster network setup in its first phase, because the perfect targeting of antennas could be done remotely with much more precision; during its life, moreover, the network's mesh could be changed, amplified or optimised without any effort.

This kind of network introduces the possibility to schedule self-running test routines during non-productive times. For example, periodically during the night, the network could run a procedure that test itself to find the most performing configuration; tests could be done to find alternative topologies, to find weaknesses in the structure, to optimize the network after an upgrade ecc.

When a crucial node fails, static networks could be heavily damaged. If the event don't cause the fracture of the WMN in more disconnected islands, it could cause the creation of a bottleneck that will slow down the local area and, consequently, the entire network. Dynamically change the topology could be a good solution, permitting a better distribution of the traffic, less local overload and, in some cases, avoid the fracture of the network.

In summary, dynamic networks provide generally:

- easier and faster setup
- more control and reliability of the network
- very high testability
- performance optimization.

2.2.3 Benefits for WCN

This project was born initially to satisfy some needs of an Italian wireless community network: Ninux.

In Ninux, like in the vast majority of WCNs in the world, mesh networks are built and maintained by volunteers. In these networks directional antennas are often the best option, since long-distance links are very common. This also explains why WCN nodes are typically mounted onto roofs, pylons or some other kind of tall structures.

Unlike in industrial facilities, common people often lack of appropriate safety devices. Mounting and orienting antennas are not simple tasks, and could became very dangerous for inexperienced workers.

Once mounted, the hope is there won't be problems to be fixed manually for a long time; but in WCN antennas are always mounted outside, subject to atmospheric agents and animals. Furthermore, some unexpected obstacles could black out the transmission (e.g. grown trees, cranes, reflecting or disturbing devices ecc.). There are a lot of reasons why community network's topology sometimes needs to be modified, optimised or totally re-designed, and this means that someone has to climb onto the roofs again and change the orientation of every single antenna.

To make WCN growing easier, to minimise the number of high-altitude works, and to provide high flexibility to these community networks, a self-turning antenna could be an excellent solution.

Google Summer of Code

CHAPTER 3

The Design

This project is intended to solve particular problems in specific circumstances. Later developments evolved the original idea to make it more flexible in different situations, but some characteristics remained the same. The following pages will provide a more detailed explanation of those starting points.

For the mechanical study, made under current laws, two effects were considered: the gravity and the wind. European standards Eurocodes were used to estimate the effects of the wind.

The last part of the chapter is provided a list of constructive solutions adopted.

3.1 Design boundaries

First and foremost, The Turnantenna is intended to help WCN volunteers. As said in the previous chapter, WCN people could be unskilled, or be not sufficiently equipped for being able to replicate a complex structure. That is the reason why the Turnantenna must be made of very cheap and readily available hardware, and its replication should be error tolerant to construction errors [A].

It was already said that the Turnantenna will be self-rotating to get WMN dynamic. However, in practice networks are frequently suited on lands where topography is variable and, in the situation where nodes are on different altitudes, antennas needs to be tilted by a certain angle to provide an effective link. For that reason, a proper rotation of one antenna should involve two different axis: in the horizontal and vertical direction. The antenna will be able to turn up to 180 degrees and 13 degrees respectively [B].

Another consideration comes from a common manufacturing practice. For directional antennas like the one used for this project, the most typical attaching points are vertical poles. Antennas have a particular shape that makes easy the fixing to a tube-like support. Since the system discussed here is an upgrade of that, it was decided to preserve this characteristic in order to maintain compatibility with older systems [C].

The intent of the project is to make the Turnantenna system usable almost everywhere. The most significant environmental aspect is the wind, so it was assumed that the worst working conditions correspond to a wind blowing at 37,5 m/s (135 km/h) [D].

Some other requisites comes from a practical consideration. The Turnantenna is designed to host different antenna models, but, at the moment, this study is based on a particular one: the Ubiquity NanoStation M5 which weights 400g,

is 80mm wide, 294mm high, and 65mm deep. All the forces and the stresses are a correlate with the specific geometry of this antenna [E].

Lastly, one important feature is the cable management of the electronics. In Ninux, like in many other WMN, the node configuration follows the "ground routing" scheme: that imply the presence of a single cable that runs from the router to the Turnantenna, which both bring signals to the antenna and power to the electronics. More information about the ground routing could be found in the next sub-chapter.

Such a configuration can be set up using a power over Ethernet (POE) injector. For this project a POE injector capable of supplying 24W (1A at 24V) is used. Considering a power consumption of 12W for the NanoStation antenna and 5W for the single-board computer (for more details on the electrical scheme see the next chapter "*Adopted solutions*"), the remaining 7W shall be sufficient for both the engines [F].

3.1.1 Ground routing[1]

Ground routing in a WMN is a node configuration where all the traffic activity is managed by a daemon that is installed in a single device, called *ground router*.

In multitasking computer operating systems, a daemon is a computer program that runs as a background process, rather than being under the direct control of an interactive user[2].

Practically, in ground routing all the network administration (like decision-making about the best route to follow to send a packet from A to B, error handling, reaction to unexpected mesh changes, ecc.) is performed by the ground router while the antenna works just like a repeater, and it can only send or receive data without having any decision-making power.

This is a Ninux community choice, since the routing daemon could be installed in the antenna firmware; doing this, part of traffic management could be performed by the antenna. Therefore, in this second scenario antennas play an active role in the route-decision computing.

Ground routing is a good choice for different reasons:

1. flexibility for the hardware adopted: for the reasons listed before, router and antennas choice is almost free. Firmware and routing protocols could be adopted according to personal needs without the necessity of dealing with software compatibility with the preferred networking daemon;
2. performances: in ground routing there is a single daemon instance per router; in other schemes there are one per antenna. In this second case, number of players in the routing management play increases exponentially, producing a significantly decrease of the entire network performance. That happens every time a network event occurs (like a node get off) and all the managing actors have to have learned about this. The more are the actors, the more is the internal traffic produced to reach everyone, and the less are the unallocated resources available for network users.
3. flexibility of the network: antennas and routers have very different computational capabilities. If antennas host the networking daemon, they could contain a smaller number of features due to the minor memory and less data processing capability of the antenna. Moreover, antennas are onto roofs, pylons or others; routers are into houses and offices instead. When it comes the time of making a big change in the meshing devices, the effort to reach the ones or the others will be significantly different.

[1] Ninux, "Ground Routing HowTo", Ninux.org
[2] LINFO, "Daemon Definition", 2005

3.2 Norms

The effect of the wind is calculated according to the *Eurocode 1*[3], following the guidelines indicated in the Leonardo da Vinci Pilot Project's handbook[4]. In this study the wind will be considered quasi-static, namely without taking into account dynamic and aeroelastic effects.

3.2.1 Peak wind pressure

One of the main parameters in the determination of wind actions on structures is the characteristic peak wind pressure q_p, which is influenced by local factors (e.g. terrain roughness and orography/terrain topography) and the height above terrain. The peak wind pressure accounts for the mean pressure (basic pressure) and a turbulence component.

To find q_b, v_p has to be evaluated first with the following formula.

$$v_b = c_{dir} \cdot c_{season} \cdot v_{b,0}$$

The fundamental value of the basic wind velocity, $v_{b,0}$, is the characteristic 10 minutes mean wind velocity, irrespective of wind direction and time of year, at 10m above ground level in open country terrain with low vegetation such as grass and isolated obstacles with separations of at least 20 obstacle heights. These characteristic values correspond to annual probabilities of exceedence of 0,02 which corresponds to a return period of 50 years.

The norm distinguish situations where the wind has a particular prevalent direction, and where its speed changes seasonally. In this project, due to the unpredictability of those factors, either the coefficients c_{season} will be taken unitary.

The following relationship exists between the basic velocity and the basic pressure:

$$q_b = \frac{\rho}{2} \cdot v_b^2$$

where ρ is the air density (can be set to 1,25 kg/m^3)

The basic value of the velocity pressure has to be transformed into the value at the reference height of the considered structure. Velocity at a relevant height and the gustiness of the wind depend on the terrain roughness. The roughness factor describing the variation of the speed with height has to be determined in order to obtain the mean wind speed at the relevant height. Note that the Eurocode 1 maximum value for the height is 200 m [G].

The roughness factor related to a minimum height z_{min} for the calculation is:

$$c_r(z) = k_r \cdot ln\left(\frac{z}{z_0}\right), \quad \text{but} \quad z \geq z_{min}$$
$$k_r = 0,19 \cdot \left(\frac{z_0}{z_{0,II}}\right)^{0,07}$$

where:

- k_r = terrain factor
- z_0 = roughness length
- z_{min} = minimum height
- $z_{0,II} = 0,05\ m$ (terrain category II, Table 2.1)

[3] European Union, "Eurocode 1: Actions on structures - Part 1-4: General actions - Wind actions" (EN 1991-1-4), 2005
[4] Leonardo da Vinci Pilot Project, "Handbook 3 Action effects for buildings", 2005, CZ/02/B/F/PP-134007 26.7.2017

Terrain category	Characteristic of the terrain	z_0[m]	z_min[m]
0	sea or coastal area	0,003	1,0
I	lakes; no obstacles	0,01	1,0
II	low vegetation; isolated obstacles with distances of at least 20 times of obstacle heights	0,05	2,0
III	regular vegetation; forests; suburbs; villages	0,3	5,0
IV	at least 15% of the surface covered with buildings with average height of at least 15 m	1	10,0

Table 2-1 Terrein categories

In case of general assumption, the gust pressure (or peak pressure) $q_p(z)$ at the reference height of the considered terrain category is calculated with the:

$$q_p(z) = q_b \cdot c_r(z)^2 \cdot \left[1 + \frac{7}{ln\left(\frac{z}{z_0}\right)}\right]$$

Given the uncertainty of both the wind conditions and environment where the Turnantenna will be mounted, to find a design value for the peak pressure will be considered the worst reasonable case.

The basic speed was specified before *[D]*; the height above terrain is taken pair to the maximum permissible value *[G]*, and it was considered that the strongest wind is felt in open lands:

$v_b = 37,5\ m/s$

$z = 200\ m$

$Terrain\ category = 0$

Now, following the previous proceeding, the peak wind pressure could be easily found:

$q_p = 4300 \frac{N}{m^2}$

As next step, the norm suggests to correct this value in case of particular stressing situations (e.g. buildings on top of hills and ridges, surrounding constructions that work like convergent nozzles, ecc.). However, in this case there is no possibility to take into account all the random peculiarities of all the different possible scenarios, but is not even possible to exclude such of situations.

A better option is to consider the values of the mean speed indicated by the European wind Atlas[5], which subdivides the European territory in five zones. The following map (Figure 2-1 Distribution of wind resources in Europe. By means of the legend the available wind energy at a height of 50 metres can be estimated for five topographic conditions. Regions where local concentration effects may occur are not indicated.) resumes those values:

In the atlas, the maximum speed value is 11,5 m/s. The design wind speed is 37,5 m/s *[D]* instead. The safety coefficient results over than 3,2. This is considered enough to conclude that the peak pressure was determined with an appropriate safety margin.

3.2.2 Wind Forces

In simplified terms, the force exerted by the wind on the antenna is given by:

$$F_w = q_p \cdot A \cdot C_f$$

[5] Troen Ib, Lundtang Petersen Erik, "European Wind Atlas", 1989, ISBN 87-550-1482-8

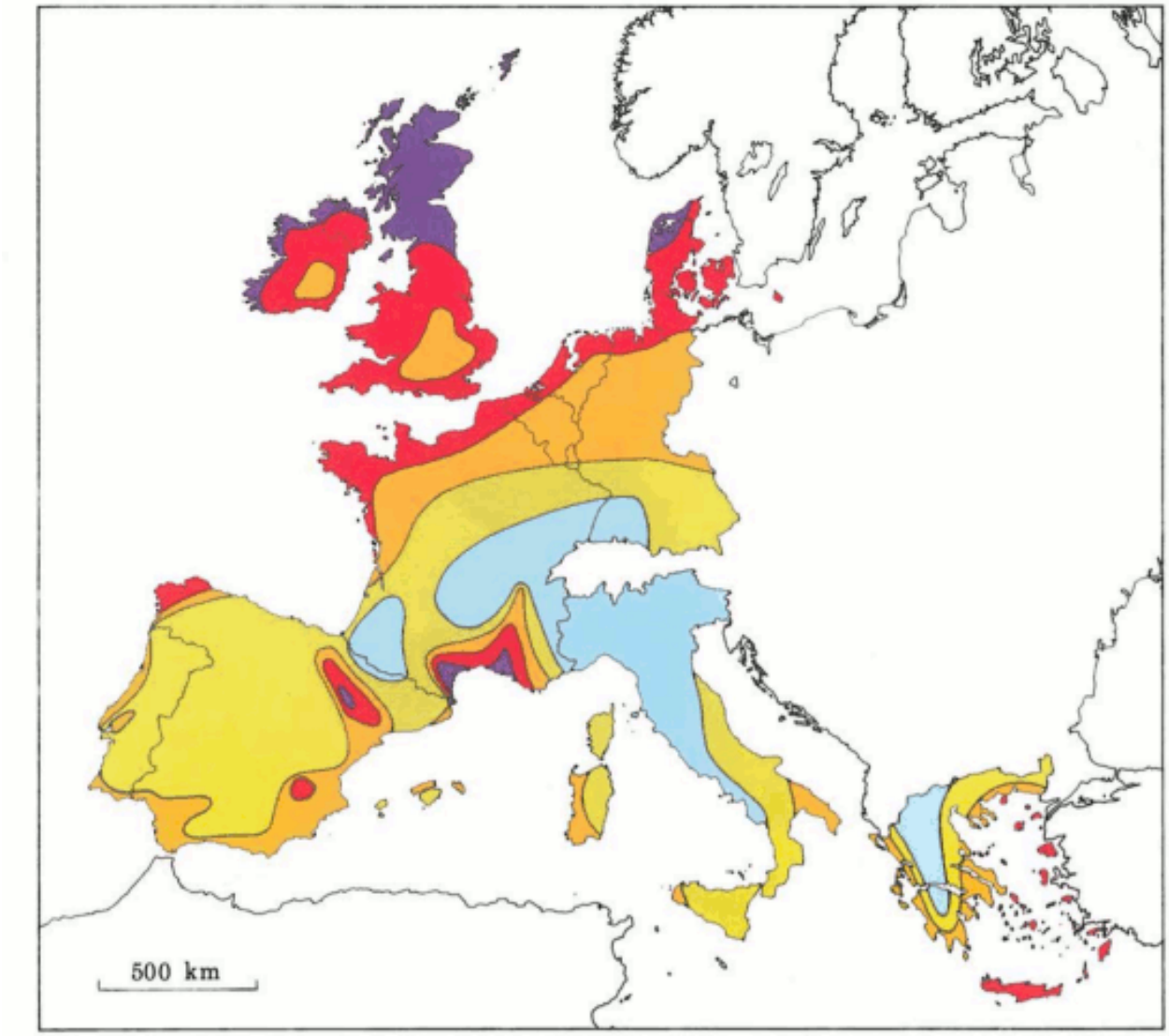

Wind resources[1] at 50 metres above ground level for five different topographic conditions

	Sheltered terrain[2]		Open plain[3]		At a sea coast[4]		Open sea[5]		Hills and ridges[6]	
	$m\,s^{-1}$	Wm^{-2}	$m\,s^{-1}$	Wm^{-2}	$m\,s^{-1}$	Wm^{-2}	$m\,s^{-1}$	Wm^{-2}	$m\,s^{-1}$	Wm^{-2}
	> 6.0	> 250	> 7.5	> 500	> 8.5	> 700	> 9.0	> 800	> 11.5	> 1800
	5.0-6.0	150-250	6.5-7.5	300-500	7.0-8.5	400-700	8.0-9.0	600-800	10.0-11.5	1200-1800
	4.5-5.0	100-150	5.5-6.5	200-300	6.0-7.0	250-400	7.0-8.0	400-600	8.5-10.0	700-1200
	3.5-4.5	50-100	4.5-5.5	100-200	5.0-6.0	150-250	5.5-7.0	200-400	7.0-8.5	400-700
	< 3.5	< 50	< 4.5	< 100	< 5.0	< 150	< 5.5	< 200	< 7.0	< 400

Fig. 1: Figure 2-1 Distribution of wind resources in Europe. By means of the legend the available wind energy at a height of 50 metres can be estimated for five topographic conditions. Regions where local concentration effects may occur are not indicated.

C_f is the force coefficient, the equivalent of the drag coefficient known in fluid dynamics. The Eurocode 1 gives the following definition:

$$C_f = C_{f,0} \cdot \Psi_f$$

where:

- $C_{f,0}$, is the force coefficient of a rectangular section with sharp corners and without free-end flow, as given by the Figure 2-2.
- Ψ_f is the reduction factor for square sections with rounded corners, Figure 2-3.

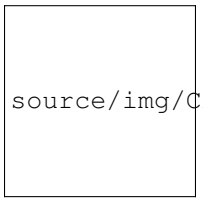

Fig. 2: Figure 2-2 Force coefficients of rectangular sections with sharp corners and without free end flow

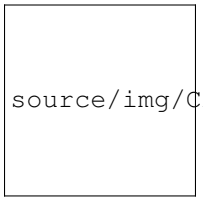

Fig. 3: Figure 2-3 Reduction factor for a square cross-section with rounded corners

The antenna has the following dimensions:

The wind could blow either frontal or by side, so the two cases will be studied separately.

Starting from a frontal blowing wind, the b/d ratio results to be equal to 2,6 , which determines a value of $C_{f,0}$ pair to 1,3.

With a side wind, the ratio become 0,38 , with a consequent value of 2,1 for the force coefficient.

The shape of the antenna is asymmetric, and is neither a square nor a rounded shape. For that reason, the reduction factor could be considered as the mean of the two mid-shapes. For a perfect square section the factor is unitary, while for the rounded corners case ($r = 15\ mm$) it results pair to 0,5. The mean value is 0,75.

The global force coefficient, in the worst case, is:

$$C_f = 2,1 \cdot 0,75 = 1,6$$

3.3 Stress analysis

In this section the effects of the external forces will be evaluated to find all the critical points, and to provide a magnitude of the stress that every component will have to resist to.

First of all, the forces will be discussed and estimated; after that, a general analysis of the distribution of the internal forces will be presented to provide a set of equations useful to find forces and moments in all the structure. The reason of this approach is that the Turnantenna is open source, and everyone shall be free to build it in different ways with different dimensions, but still having the possibility to benefit from this work. Lastly, most critical pieces will be verified.

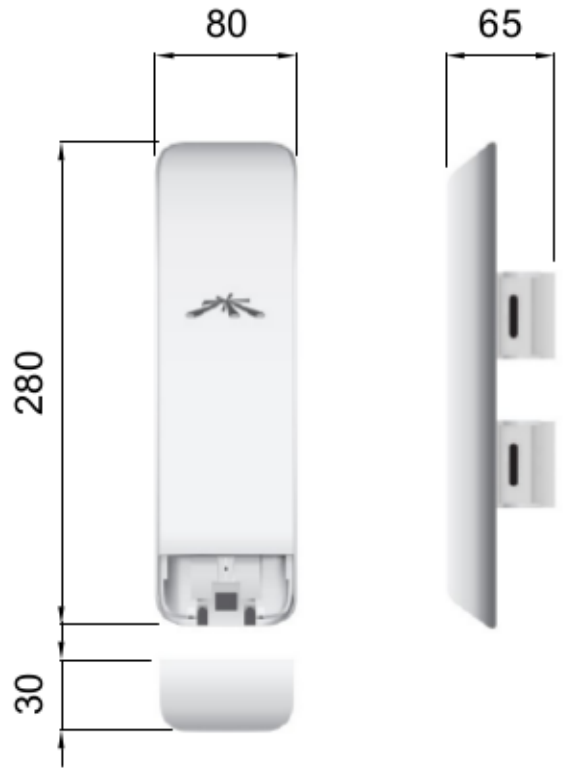

Fig. 4: Figure 2-4 Ubiquity NanoStation M5 dimensions (mm)

3.3.1 Definitions

The antenna must be able to rotate around two axis *[B]*. The figure below shows the scheme of the system. Points E and F are fixed, and are cylindrical joints that allow the rotation of the rotating frame (A-B-C-D) around the vertical axis.

The two engines are hosted in A and E; B and C correspond to the attaching points of the antenna to the four-bar linkage.

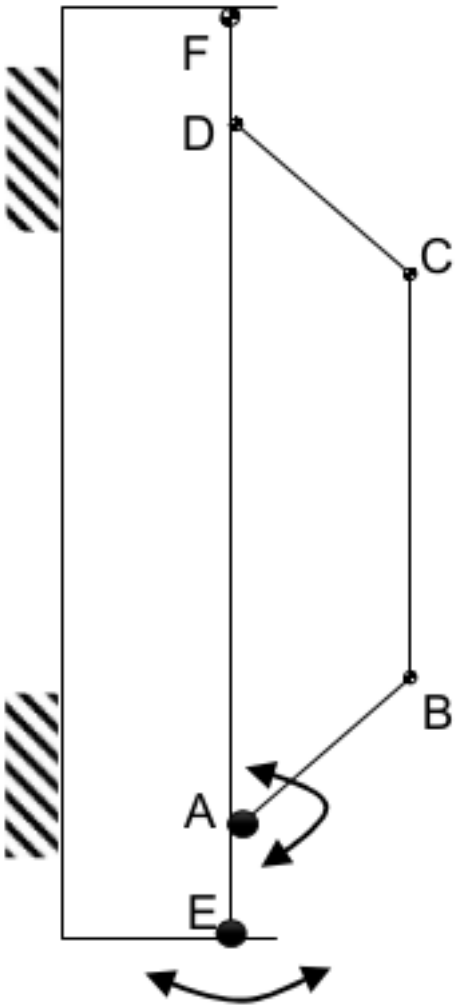

Fig. 5: Figure 2-5 Scheme of the Turnantenna. E-F frame is fixed; A-B-C-D can rotate around the vertical axis; C-B are the fixing points of the antenna, and have 2 degrees of freedom.

The hatches represent the fixings to a tube-like support *[C]*.

3.3.2 External forces evaluation

Using the *Eurocode* approach, it was possible to find the pressure of the wind and the drag coefficient. In the most general case, the wind could blows in all directions. Furthermore, wind from both sides produces the same effects on

the structure, and rear wind could be considered basically equivalent to frontal wind. The β angle is introduced to characterize the wind direction, which is considered always horizontal; for symmetry, it's sufficient to study the effects in a quarter-turn domain.

The β angle is defined as follows:

$$\begin{cases} \beta = 0, & \text{side wind} \\ 0 < \beta < \frac{\pi}{2}, & \text{general wind} \\ \beta = \frac{\pi}{2}, & \text{frontal wind} \end{cases}$$

To evaluate the wind effects, the force it is divided into two components, one orthogonal and one tangential to the face of the antenna:

$$R_n = q_p \cdot c_f \cdot \sin\beta \cdot A_{A,n}$$
$$R_\tau = q_p \cdot c_f \cdot \cos\beta \cdot A_{A,\tau}$$

where A_n and A_τ are the frontal and the side area of the antenna; q_p and c_f are the peak wind pressure and the force coefficient found in the previous chapter.

This study is based on the following hypothesis:

- the mobile frame LEFM (Figure 2-7) is a rectangular section tube t × k;
- the force developed by the action of the wind on the rockers and the horizontal extensions of the frame is negligible:
- the antenna will be sketched as two parallelepipeds jointed together:
  - A prims with the dimensions of the antenna itself $(w_A \cdot h_A)$
  - A smaller one that takes into account the contribute of the two supports $(w_A \cdot h_A)/2$

To make it clear, the sketch used to perform the calculus is shown in Figure 2-7 , while the real mobile frame is very similar to Figure 2-6.

The vertical axis of rotation is in the middle between the vertical face of the frame and the antenna. The pressure acting on these two areas will cause the birth of two parallel forces with opposite direction. That's why the two areas need to be considered separately.

Areas values result:

$$A_{A,n} = b_A \cdot h_A$$
$$A_{\tau_1} = A_{A,\tau} + A_{Supports,\tau} = w_A \cdot h_A(1 + 0,5)$$
$$A_{\tau_2} = A_{Frame,\tau} = \overline{EF} \cdot t$$

The weight of the entire system will be evaluated approximately, since there is not a definitive constructive solution. The antenna mass is 400g *[F]*. It is supposed that, together with the rockers, it will reach 1kg. The mobile frame is supposed to have the same mass of the antenna group, and the fixed one the double of this quantity:

$m_A = 1\ Kg$

$m_M = 1\ Kg$

$m_F = 2\ Kg$

3.3.3 Static analysis

The following part will discuss the distribution forces and moments over the Turnantenna structure for all the configurations determined by the pitch angle θ, without specifying any geometrical information. All the expressions will be given in their general form and, only after, final results will be listed.

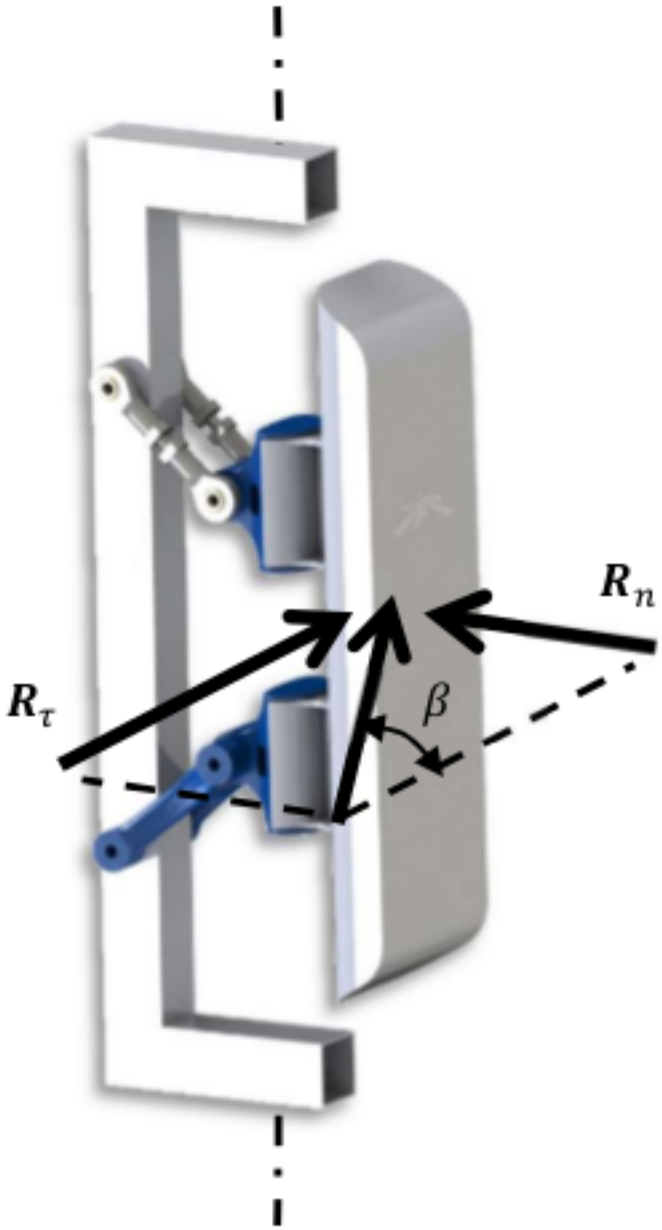

Fig. 6: Figure 2-6 Explanation of the β angle

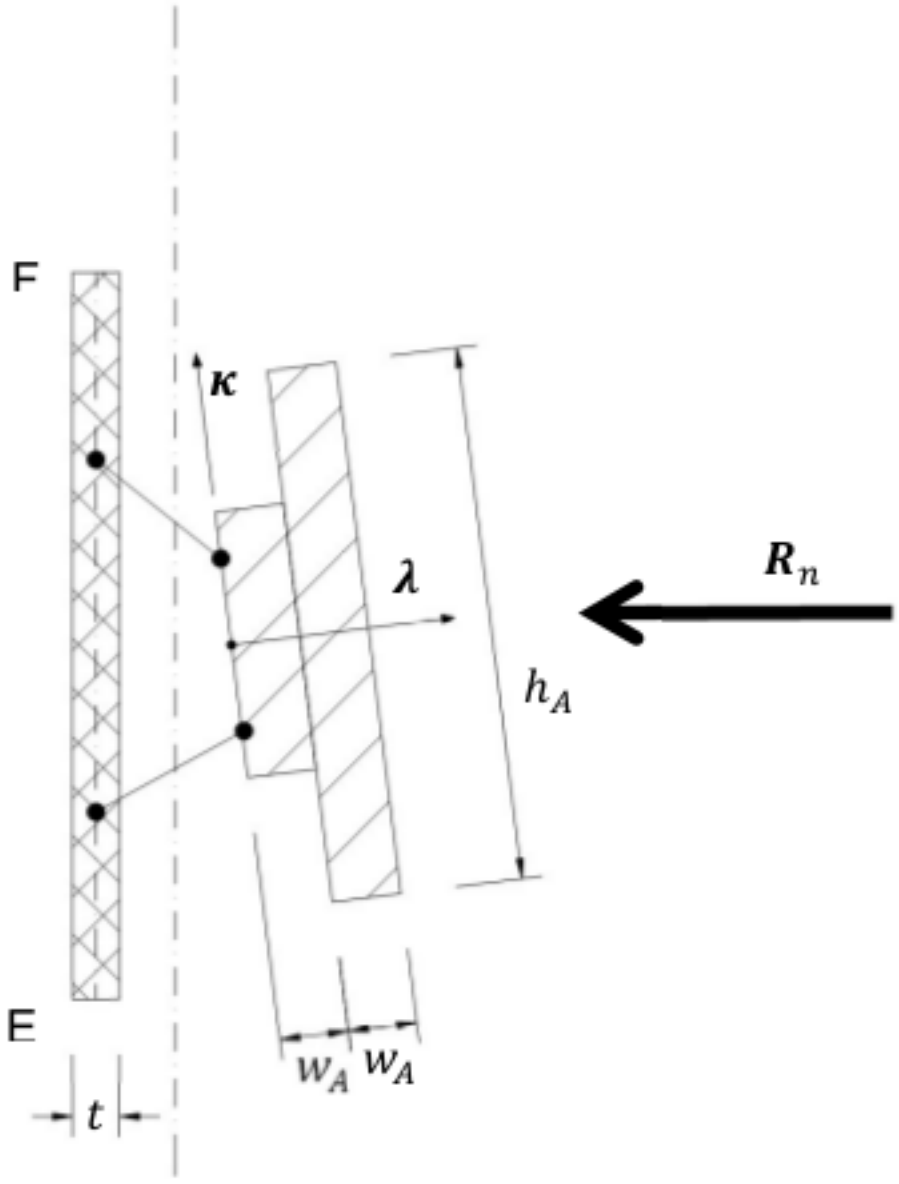

Fig. 7: Figure 2-7 Schematic representation of the mobile frame used to calculate the side wind forces

On first examination, the wind direction will be considered perfectly frontal $\beta = \frac{\pi}{2}$ with the only effects induced by R_n. Later, a tangential component will be added, and evaluated.

Frontal wind

The wind is considered perfectly frontal. That means that angles have the following values:

$$\begin{cases} \theta \in [-6, 7] \\ \beta = \frac{\pi}{2} \end{cases}$$

The external forces here are:

- $W_A = m_A \cdot g \approx 10\ N$
- $W_M = m_M \cdot g \approx 10\ N$
- $R_n = q_p \cdot c_f \cdot A_{A,n} = 4300\ \frac{N}{m^2} \cdot 1,6 \cdot 0,294\ m \cdot 0,08\ m \approx 160\ N$

A more detailed scheme of the Turnantenna, which has a shape similar to the one illustrated in Figure 2-6, is shown in Figure 2-8. In a first approximation all the elements could be idealised as rigid beams.

Beam 1

The first beam, as shown in Figure 2-9, is subjected to four forces: the weight of the antenna W_A, the effect of the wind pressure R_n, and the internal forces F_{21} and F_{31}.

The bar number 2 is hinged on both the ends, consequently F_{21} corresponds to the physical angle γ. The force F_{31} will have its same direction, that is not align with the beam 3; it's identified by the angle ϕ which has not a direct connection with the physical angle δ.

The following equations are valid since the beam is in a state of equilibrium:

$$\begin{aligned} x] \quad & F_{21} \cdot \sin\gamma + F_{31} \cdot \sin\varphi = R_n \\ y] \quad & F_{31} \cdot \cos\gamma = P_A + F_{21} \cdot \cos\varphi \\ M_{(B)}] \quad & R_n \cdot \tfrac{h}{2} \cdot \cos\theta - P_A \cdot \tfrac{h}{2} \cdot \sin\theta - F_{21} \cdot h \cdot \sin(\gamma + \theta) = 0 \end{aligned}$$

which can give the following expressions:

$$\begin{aligned} F_{21} &= \frac{\frac{R_n}{2} \cdot \cos\theta - \frac{P_A}{2} \cdot \sin\theta}{\sin(\gamma + \theta)} \\ F_{31} &= \frac{R_n - F_{21} \cdot \sin\gamma}{\sin\varphi} \\ \varphi &= \arctan\left(\frac{R_n - F_{21} \cdot \sin\gamma}{P_A + F_{21} \cdot \cos\gamma}\right) \end{aligned}$$

Bar 2

This bar has revolute joints on both the ends, and it results to be compressed. The only two forces applied are equal in magnitude and opposite in direction. As clarified in Figure 2-10, the equilibrium gives:

$$F_{42} = F_{12} = F_2$$

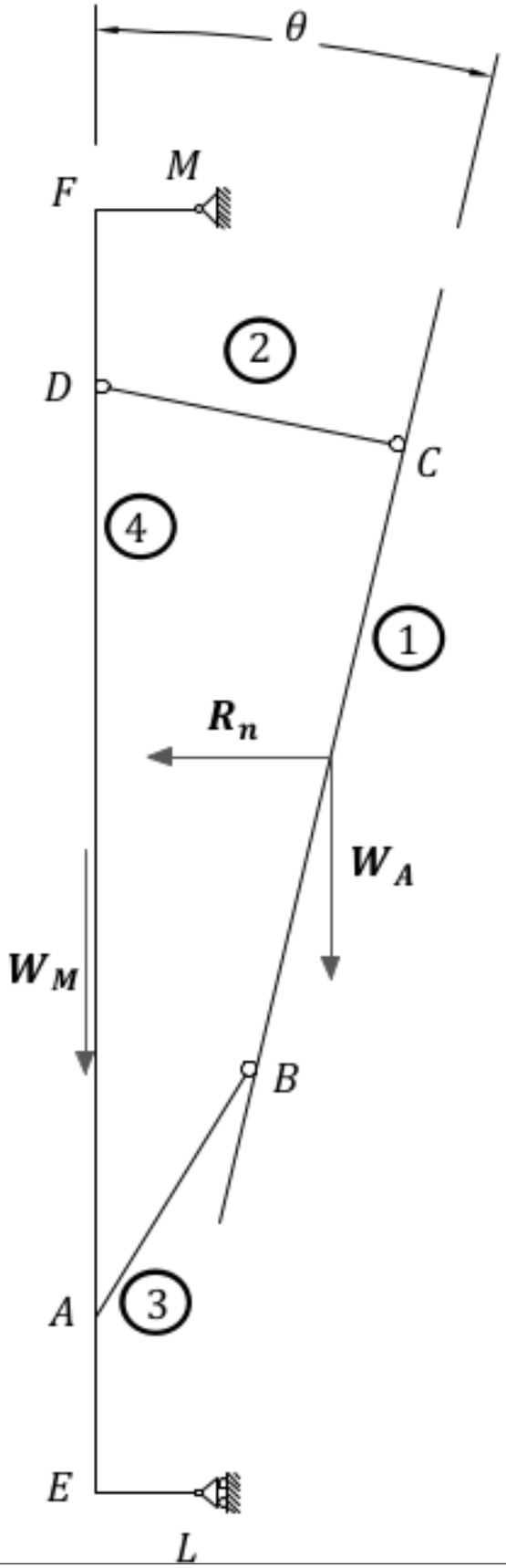

Fig. 8: Figure 2-8 Scheme of the Turnantenna: the mobile frame assembly

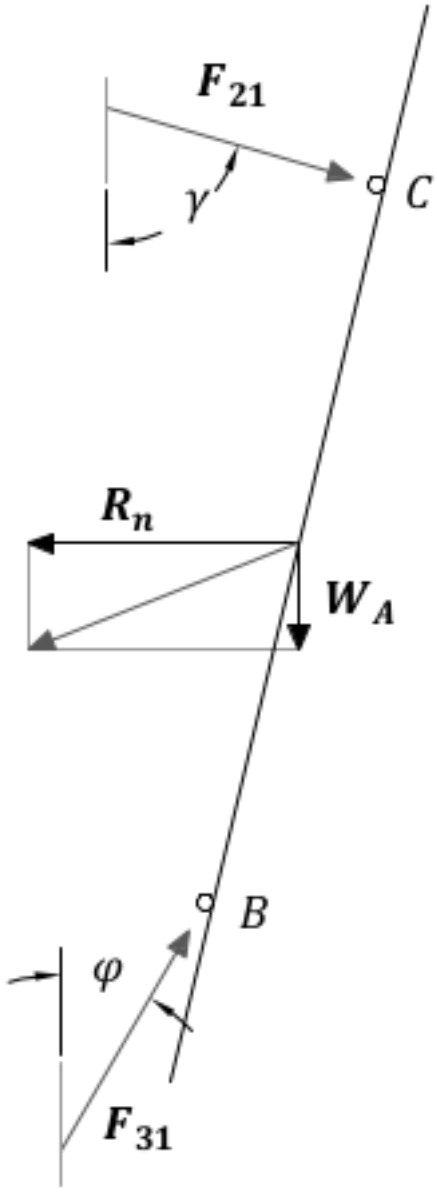

Fig. 9: Figure 2-9 Beam 1

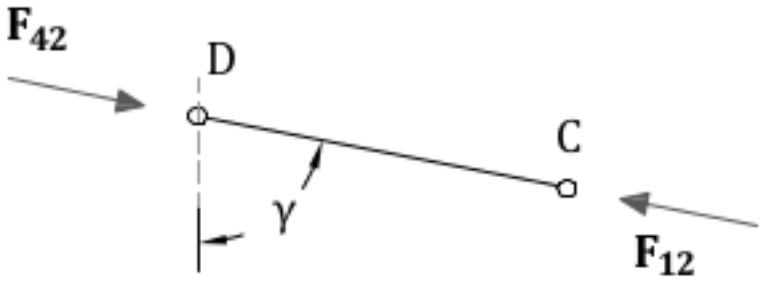

Fig. 10: Figure 2-10 Bar 2

Beam 3

The third beam is hinged on both the sides, but in the point A the engine apply a moment to the beam to hold it in position. The two internal forces will be mutually parallel, and will apply a torque balanced by the engine (Figure 2-11), which could be calculated as:

$$C_1 = F_{13} \cdot l \cdot \sin(\varphi - \delta)$$

More equations come from the same hypothesis of balance:

$$\begin{aligned} F_{43} &= F_{13} = F_3 \\ F_{3\perp} &= F_3 \cdot \sin(\varphi - \delta) \\ F_{3\parallel} &= F_3 \cdot \cos(\varphi - \delta) \end{aligned}$$

$F_{3\perp}$ and 3 $F_{3\parallel}$ are the components of the force F_3 perpendicular and parallel to the beam 3, and C_1 is the estimate of the real torque that the first engine has to bear when the wind blows at 37,5 m/s.

Beam 4

Looking to the beam 4 scheme in Figure 2-12, the following equations could be written

$$\begin{aligned} x] \quad & H_L + H_M = F_{34} \cdot \sin\varphi + F_{24} \cdot \sin\gamma \\ y] \quad & V_M = W_M + F_{34} \cdot \cos\varphi - F_{24} \cdot \cos\gamma \\ M_{(F)}] \quad & V_M \cdot \overline{FM} + C_1 - F_{34} \cdot \overline{AF} \cdot \sin\varphi - F_{24} \cdot \overline{DF} \sin\gamma + H_L \cdot \overline{EF} = 0 \end{aligned}$$

From which could be obtained:

$$\begin{aligned} V_M &= W_A + W_M \\ H_L &= \frac{F_{34} \cdot \overline{AF} \cdot \sin\varphi + F_{24} \cdot \overline{DF} \cdot \sin\gamma - C_1 - V_M \cdot \overline{FM}}{\overline{EF}} \\ H_M &= F_{34} \cdot \sin\varphi + F_{24} \sin\gamma - H_L \end{aligned}$$

Where V and H are respectively the horizontal and the vertical reactions of the fixed frame constraints.

Generic wind direction

In this part, the effect of a lateral wind will be taken into account. At this point it is necessary to consider the whole effect of the wind as the β angle changes.

$$\begin{cases} \theta \in [-6, 7] \\ \beta = (0, \frac{\pi}{2}) \end{cases}$$

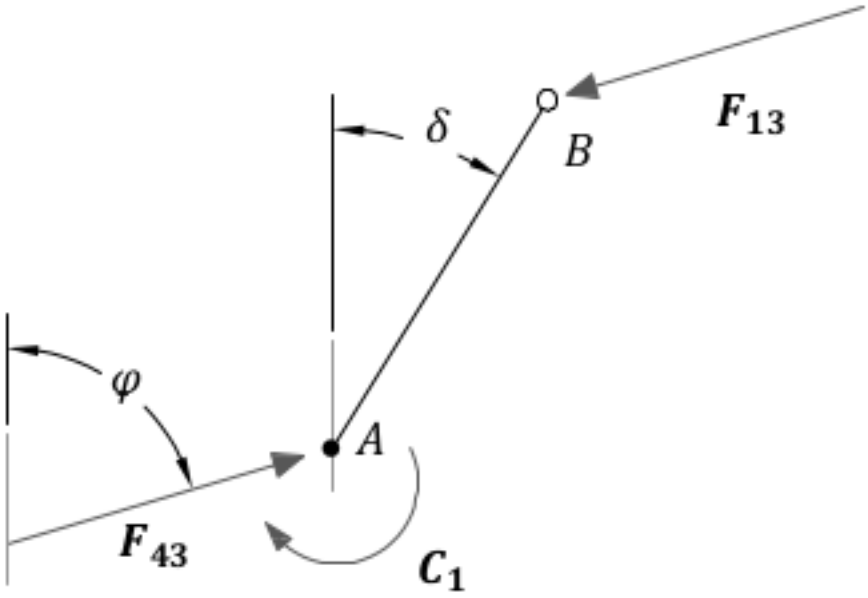

Fig. 11: Figure 2-11 Beam 3

To study the structure when $\beta\frac{\pi}{2}$, the principle of superposition of the effects allows to re-use the resulting equations of the previous part, and to sum the side wind effects in order to obtain a complete analysis.

To get the problem single-variable, the reader should know that, in the next chapter *"Internal stress determination"*, maximum stresses are obtained when the pitch angle is $\theta = -6$. This is valid for every wind speed values and for all directions.

In summary, the pitch angle will be kept fixed, while β changes, because a change in the β angle produce the exactly same output as a change in the yaw angle. Applying this approach, the study results to be very fast and with no loss of reliability.

A lateral wind cause the birth of a moment C_2 which, as C_1 , represent the torque exerted by the secondary engine to maintain the antenna in the desired position when wind blows. The characterising force of this moment is the tangential component of R , the application point distance depends on the particular geometrical schematization.

Introducing a reference system $\lambda\ \kappa$ with the origin Q placed at the centre height on the left corner of the antenna block (Figure 2-13), with the axis tilted at θ angle, positive for left-to-right and bottom-to-top directions, the λ coordinate of the centre of mass is:

$$\lambda_{G_2} = \frac{\sum_{i=1}^{N} S_{,i}}{A_{tot}} = \frac{w_A \cdot \frac{h_A}{2} \cdot \frac{w_A}{2} + w_A \cdot h_A \cdot \frac{3}{2} \cdot w_A}{\frac{w_A}{2} \cdot h_A + w_A \cdot h_A} = \frac{7}{6} w_A$$

where $S_{,i}$ is the first moment of area of each i element in the κ direction, and A_{tot} is the total area.

As said at the beginning of this chapter, C_2 is the sum of two opposite effects. The distances, that allow to calculate them, are the ones going from G_1 and G_2 to the axis of rotation, named respectively d_1 and d_2.

In x-y coordinates:

$$d_1 = \overline{FM} = \overline{EL}$$
$$d_2 = |y_{G_2}| - d_1$$

$\overline{FM}$ and $\overline{EL}$ are geometrical parameters.

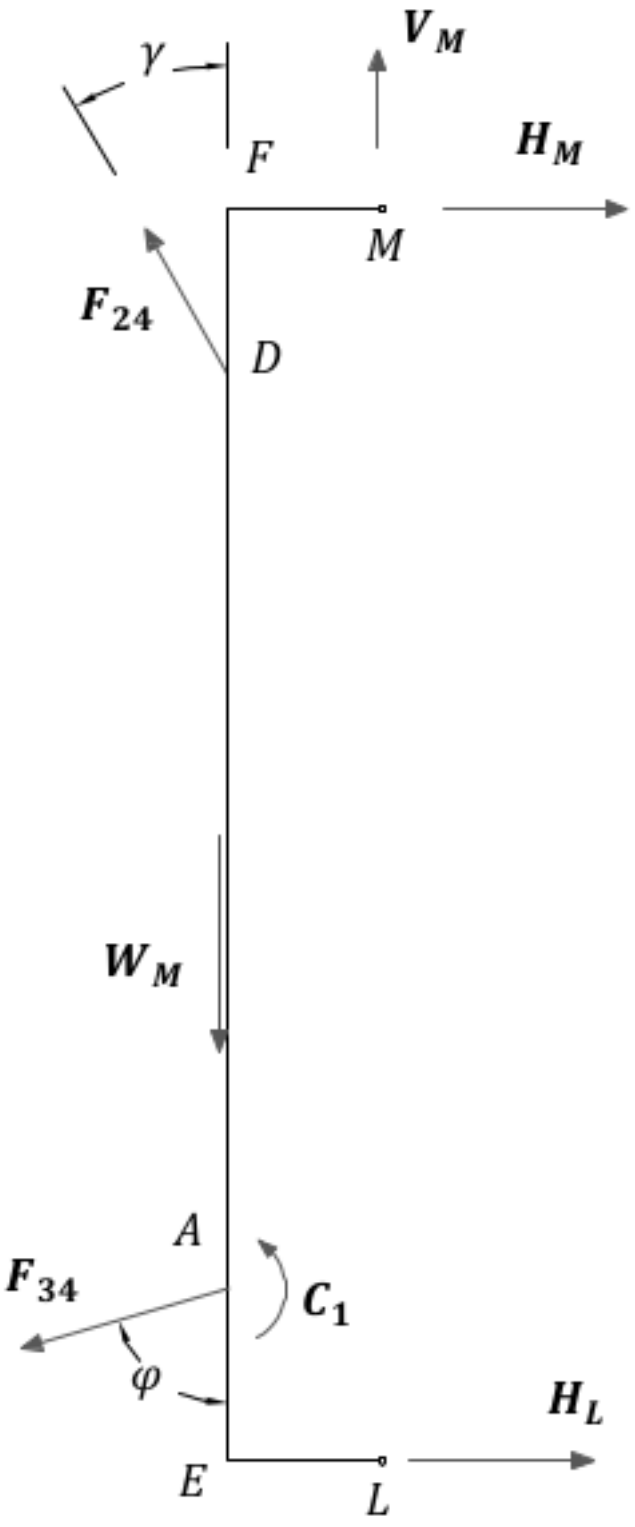

Fig. 12: Figure 2-12 Beam 4

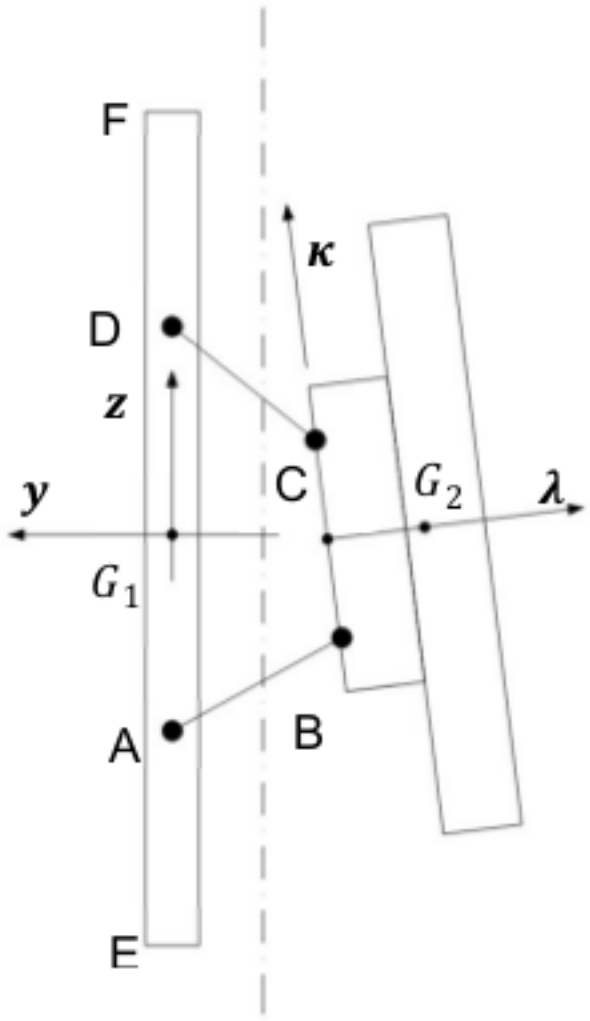

Fig. 13: Figure 2-13 Reference systems

G_1 and G_2 are defined into two different reference systems; to find y_{G_2} the λ coordinate of G should be added to the y coordinate of the centre Q, which is in the middle between B and C ($\overline{BC} = l$).

$$A \begin{cases} y_A = 0 \\ z_A = -\frac{H}{2} \end{cases} \qquad D \begin{cases} y_D = 0 \\ z_D = +\frac{H}{2} \end{cases}$$
$$B \begin{cases} y_B = y_A - l \cdot \sin\delta \\ z_B = z_A + l \cdot \cos\delta \end{cases} \qquad C \begin{cases} y_C = y_D - l \cdot \sin\gamma \\ z_C = z_D - l \cdot \cos\gamma \end{cases}$$

$$Q \begin{cases} y_Q = \frac{y_B + y_C}{2} \\ z_Q = \frac{z_B + z_C}{2} \end{cases}$$
$$G_2 \begin{cases} y_{G_2} = y_Q - \frac{7}{6} w \cdot \cos\theta \\ z_{G_2} = z_Q - \frac{7}{6} w \cdot \sin\theta \end{cases}$$

All the elements are ready. The following analysis will take into account only the effects caused by lateral winds: frontal wind and weight will be summed with the principle of superposition of the effects.

Beam 1

The first beam is connected with the third one with a revolute joint, and with the second one with a spherical bearing. Therefore, the bar 2 will not react with any force, while the third beam will exert a force and a moment.

The external force $R_{\tau,2}$ induce a rotation around a not permitted axis, hence a composite moment with both a flexural and a torsional component will stress the beam 1 (Figure 2-14).

$$F_{31} = R_{\tau,2}$$
$$M_{31f} = R_{\tau,2} \cdot \frac{h}{2}$$
$$M_{31t} = R_{\tau,2} \cdot \lambda_{G_2}$$

The vectorial sum of this two moments is:

$$M_{31} = \sqrt{M_{31f}^2 + M_{31t}^2}$$

Bar 2

The bar number two has two spherical bearings on the extremities. It has freedom to rotate around the vertical axis, and can't bear loads from the side.

Beam 3

The third beam is fastened in A to the fourth one, and has a revolute joint connection with the first one (Figure 2-15). The moment $M_{13} = M_{31}$ exerted by the beam 1 is:

$$\overrightarrow{M_{13}} = \overrightarrow{BG_2} \times \overrightarrow{R_{\tau 2}}$$

It is a vector, and its direction forms an angle α with the beam 3:

$$\alpha = \frac{\pi}{2} - \delta - (-\theta) + \varepsilon$$

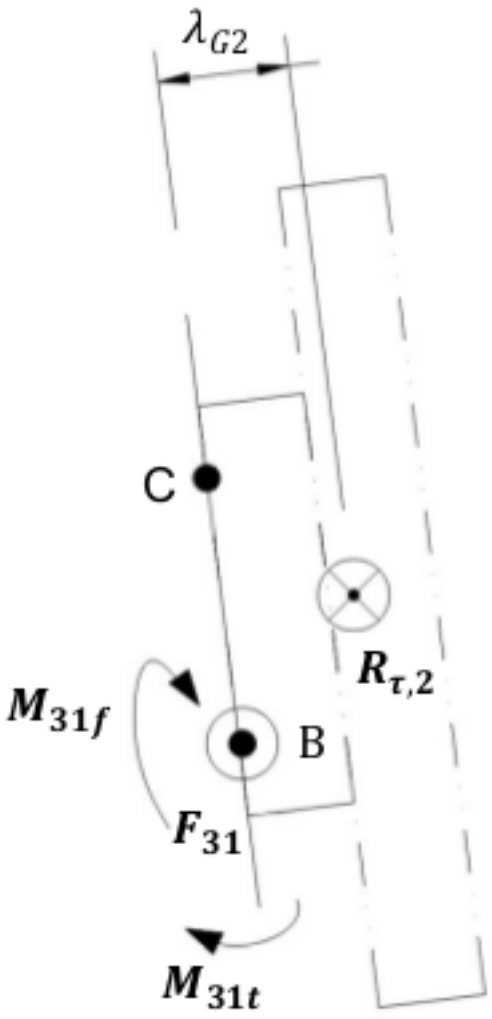

Fig. 14: Figure 2-14 Beam 1 – lateral wind

where is highlighted that θ in negative. ϵ is defined as:

$$\varepsilon = \arctan\left(\frac{\lambda_{G_2}}{\frac{h}{2}}\right)$$

Finding the components of the moment :

$$M_{13f} = M_{13} \cdot \cos\alpha$$
$$M_{13t} = M_{13} \cdot \sin\alpha$$

the following equations can be written:

$$F_{43} = F_{13}$$
$$M_{43f} = M_{13f} + F_{13} \cdot lM_{43t} = M_{13t}$$

allowing to find $M_{43} = \sqrt{M_{43f}^2 + M_{43t}^2}$. The angle between this moment and the third beam is ρ and it is:

$$\rho = \arctan\left(\frac{M_{43f}}{M_{43t}}\right)$$

Beam 4

The fourth beam has two collinear revolute joints, in L and in M. The vertical axis of rotation pass through those points. In L the engine exert a torque C_2 to keep the mobile frame still. In A, the third beam apply the moment M_34 , equal to M_43, which has a direction identified by ρ (Figure 2-16).

The flexional and the torsional components can be found with:

$$M_{34f} = M_{34} \cdot \cos\left[\rho - \left(\tfrac{\pi}{2} - \delta\right)\right]$$
$$M_{34f} = M_{34} \cdot \sin\left[\rho - \left(\tfrac{\pi}{2} - \delta\right)\right]$$

From the condition of equilibrium:

$$\begin{aligned} x] \quad & R_{\tau,1} + F_{34} = K_L + K_M \\ y] \quad & (R_{\tau,1} + F_{34}) \cdot d_1 - M_{34t} = C_2 \\ M_{\overline{FM}}] \quad & R_{\tau,1} \cdot \tfrac{\overline{EF}}{2} + F_{34} \cdot \left(\tfrac{\overline{EF}}{2} + \tfrac{h}{2}\right) - M_{34f} - K_L \cdot \overline{EF} = 0 \end{aligned}$$

the resulting equations are:

$$K_L = \frac{R_{\tau,1} \cdot \frac{\overline{EF}}{2} + F_{34}\frac{\overline{EF}+h}{2} - M_{34f}}{\overline{EF}}$$
$$K_M = R_{\tau,1} + F_{34} - K_L$$

with particular interest in:

$$C_2 = (R_{\tau,1} + F_{34}) \cdot d_1 - M_{34t}$$

To verify the outcome, the following equation provides a more direct way to calculate C_2:

$$C_2 = R_{\tau,1} \cdot d_1 - R_{\tau,2} \cdot d_2$$

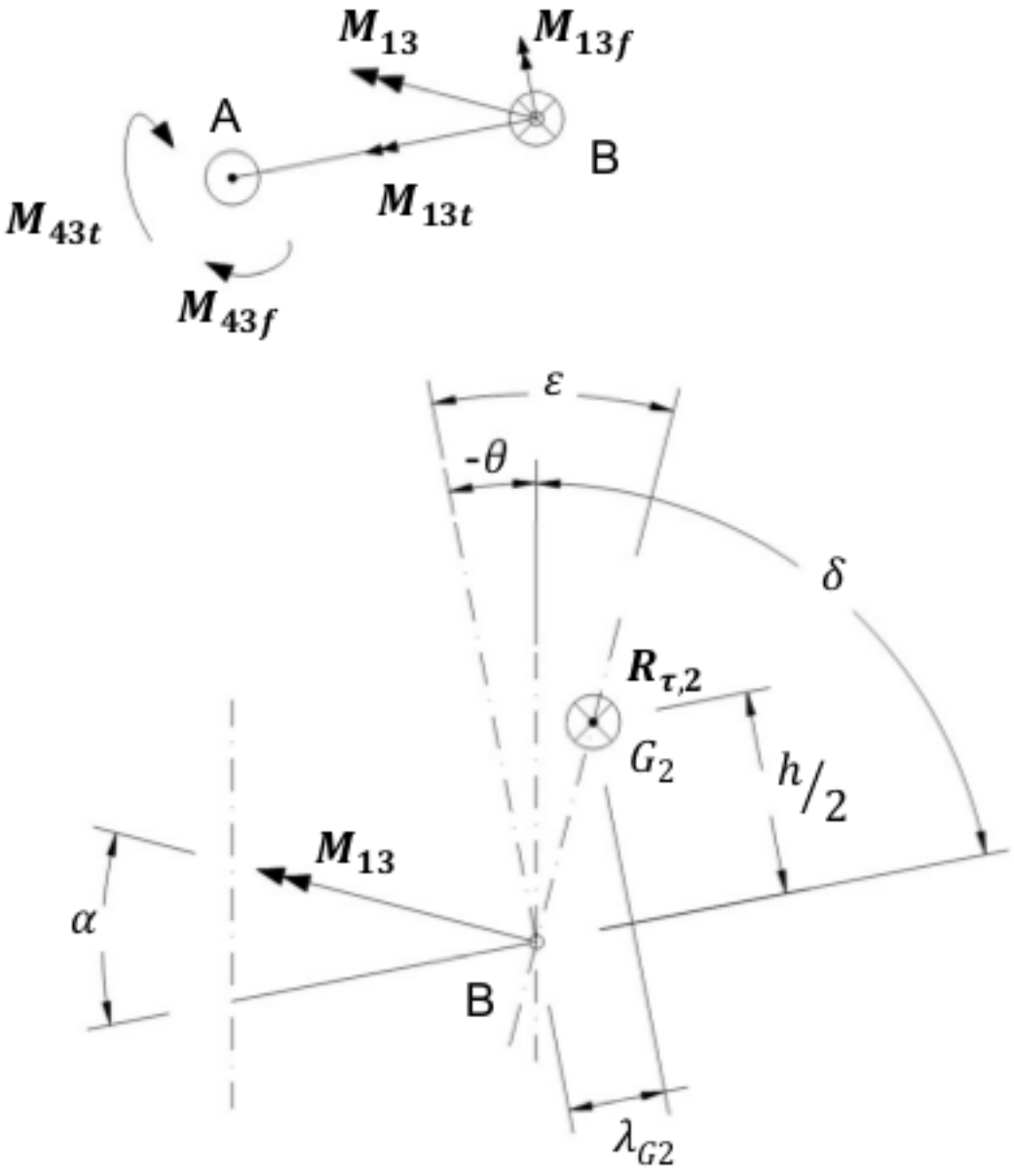

Fig. 15: Figure 2-15 Beam 3 (above) and angles definition (below) - lateral wind

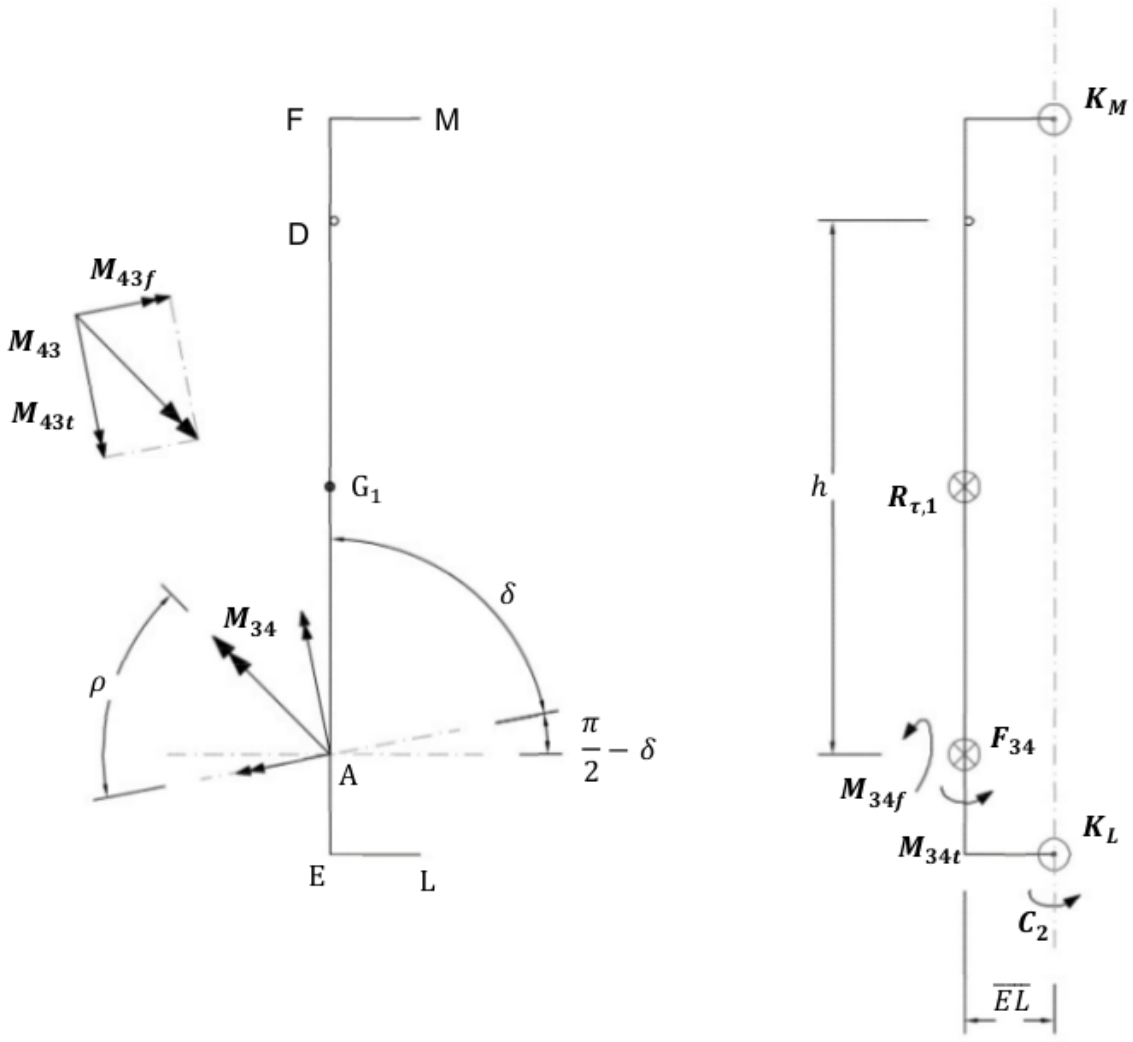

Fig. 16: Figure 2-16 Beam 4 - lateral wind

3.3.4 Internal Stress Determination

To evaluate the stresses in a real application, the following geometrical data will be assumed:

- $h = 102\ mm$
- $l = 60\ mm$
- $H = 180\ mm$
- $\overline{FD} = \overline{AE} = 95\ mm$
- $\overline{EF} = 370\ mm$
- $\overline{FM} = d_1 = 57,5\ mm$

  $\rightarrow d_2 = 22,7\ mm$
- Rectangular section aluminium tube frame $t \times k = 25 \times 25\ mm$
- Antenna's dimensions $294 \times 80 \times 31\ mm$

Note: during the following analysis, the effects of the wind on the antenna will not be taken into account, since the device is not under design, and it was not possible to access to any information about its mechanical behaviour under stress.

With a perfect frontal wind, that blows ad 37,5 m/s and develop a pressure of 4300 Pa with a drag coefficient of 1,6 , it is possible to use the equations showed in the previous chapter "*Static analysis*" to plot the following graph:

As first clear conclusion, the most critical condition appears to be the one corresponding to the angle θ = 6°. Moreover, R_n is a monotonic increasing function of the β angle, and a change of β will change the scale, but will not affect the overall trend the functions shown in the graphs above.

In light of this, it is sufficient to consider a fixed value for θ, and change β.

In these last two graphs, it emerges a practical consideration: while the particular geometry allows to have a very low torque on the second engine (C_2), the most critical component, in case of side wind, is the rocker linked to the first engine (beam 3), which has to bear the action of M_13 and M_34.

The most stressful working conditions are two:

- the one corresponding to a frontal wind: θ = 6° and β = 90°
- the one with a completely side wind: θ = 6° and β = 0

In order to give a more clear representation of the stress distribution in the following section will be shown the load charts. The first load configuration is the following:

And the corresponding load chart is the one below, where forces are expressed in N, and moments in Nm. Forces results were rounded to the nearest multiple of 5, and moments to the first decimal point.

The principle of superposition of the effects allows to study the second load configuration in a double-step procedure. Since the frontal wind is absent, the two addends of the sum will be the weight and side wind.

Using the previous graphs, it is possible to evaluate how elements of the structure are stressed.

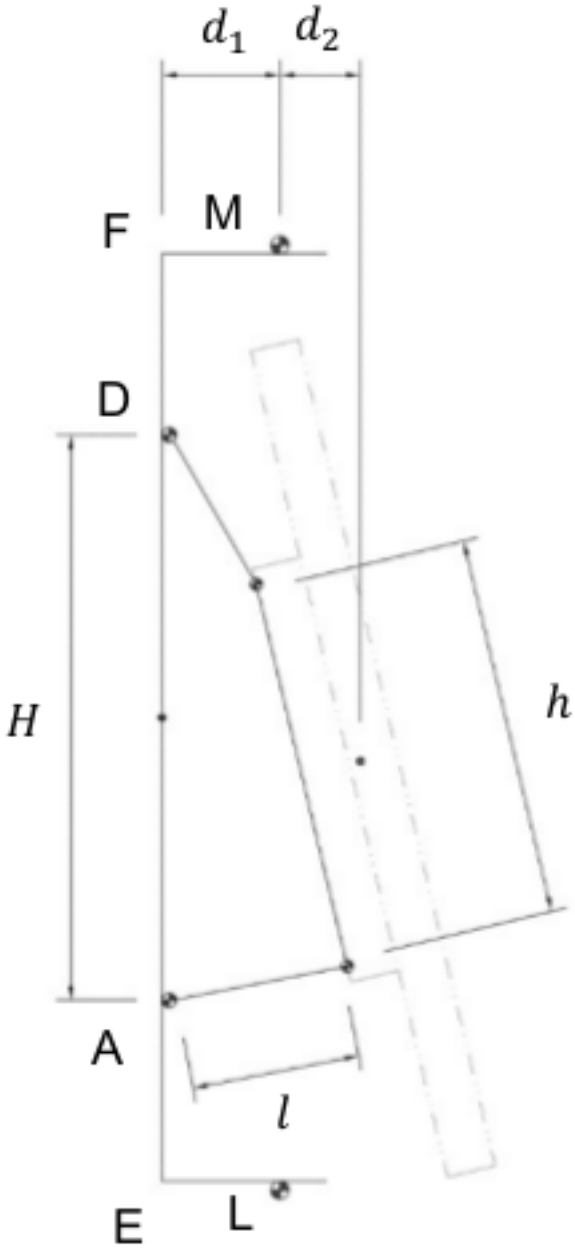

Fig. 17: Figure 2-17 Fundamental geometrical values

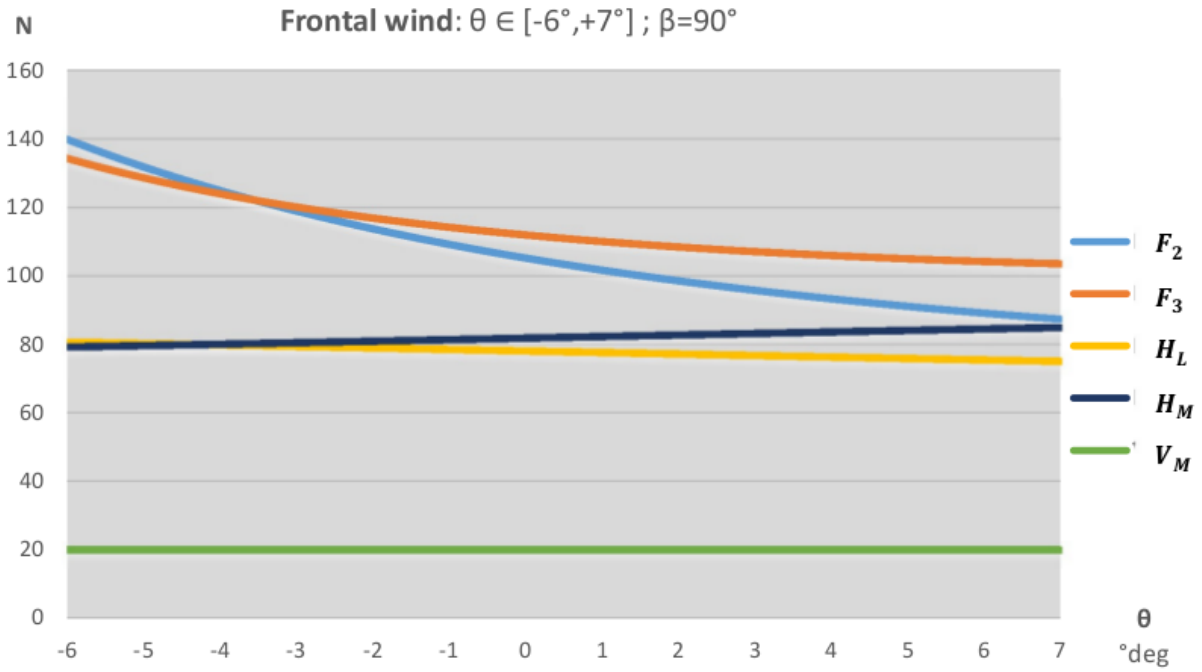
N
Frontal wind: θ ∈ [-6°,+7°] ; β=90°
160
140
120
100
80
60
40
20
0
-6 -5 -4 -3 -2 -1 0 1 2 3 4 5 6 7
θ
°deg
F_2
F_3
H_L
H_M
V_M

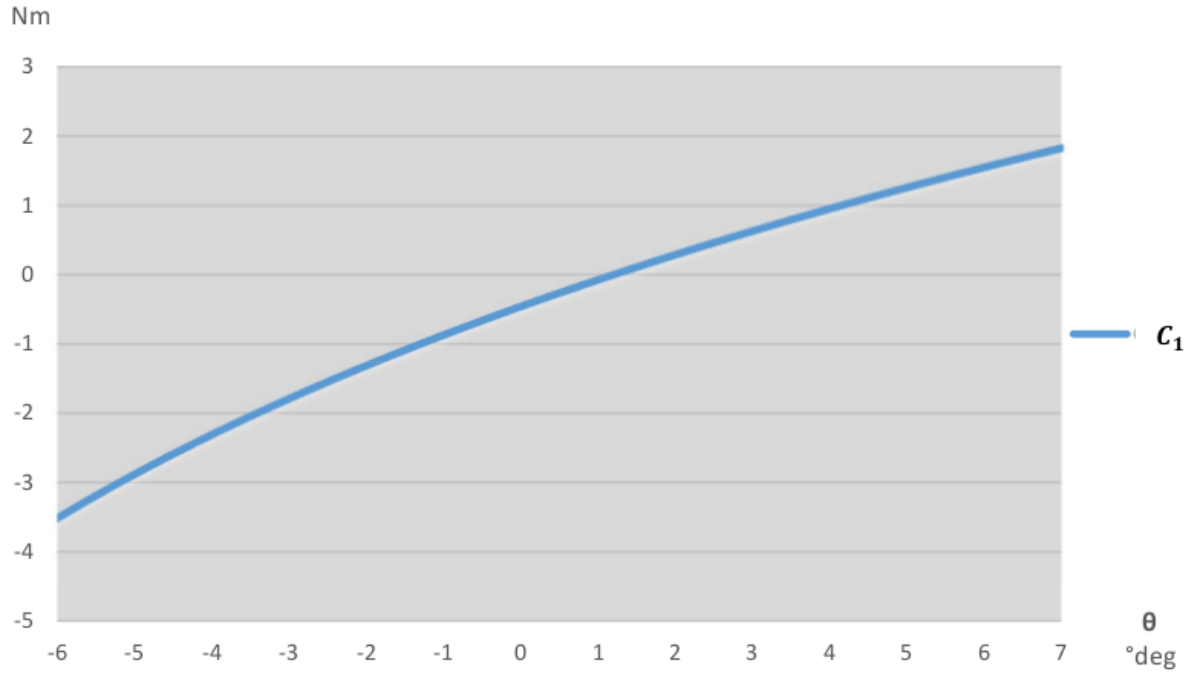
Nm
3
2
1
0
-1
-2
-3
-4
-5
-6 -5 -4 -3 -2 -1 0 1 2 3 4 5 6 7
θ
°deg
C_1

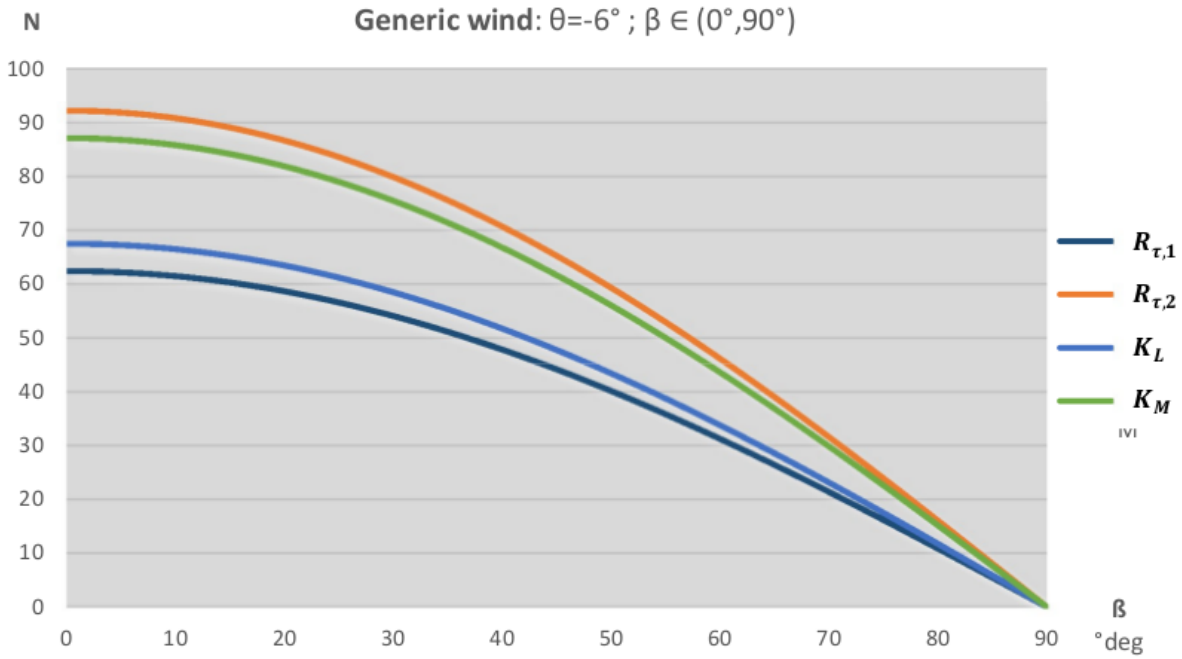
N
Generic wind: θ=-6° ; β ∈ (0°,90°)
100
90
80
70
60
50
40
30
20
10
0
0
10
20
30
40
50
60
70
80
90
ß
°deg
$R_{\tau,1}$
$R_{\tau,2}$
K_L
K_M

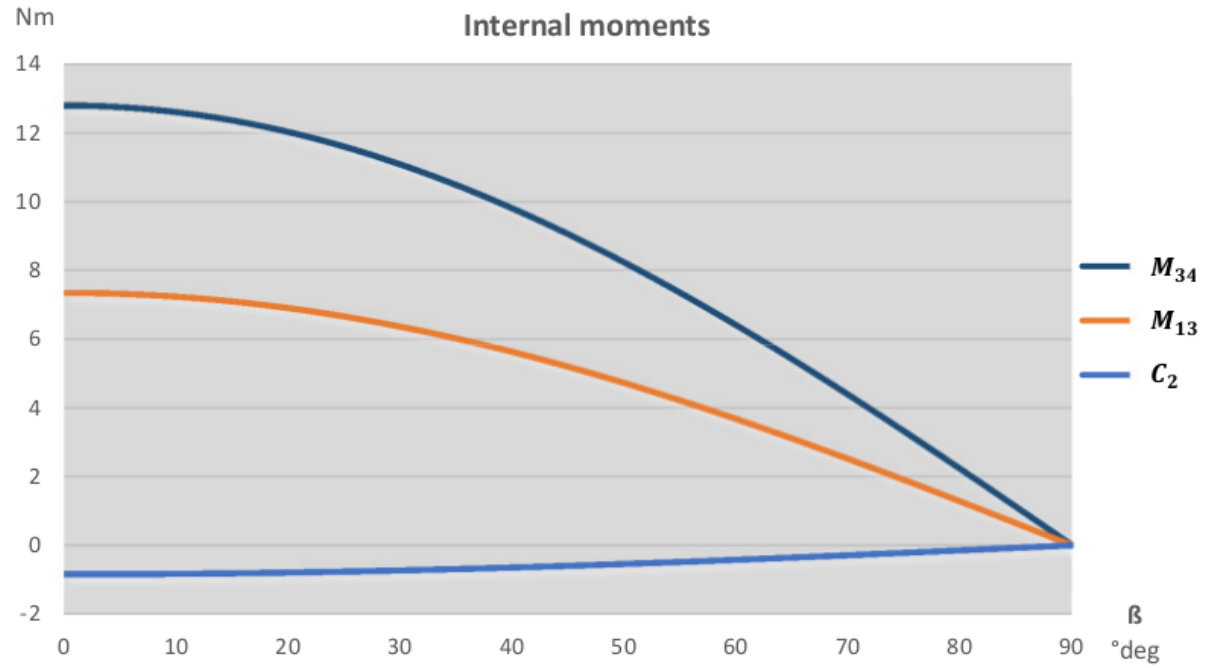
Nm
Internal moments
14
12
10
8
6
4
2
0
-2
0
10
20
30
40
50
60
70
80
90
ß
°deg
M_{34}
M_{13}
C_2

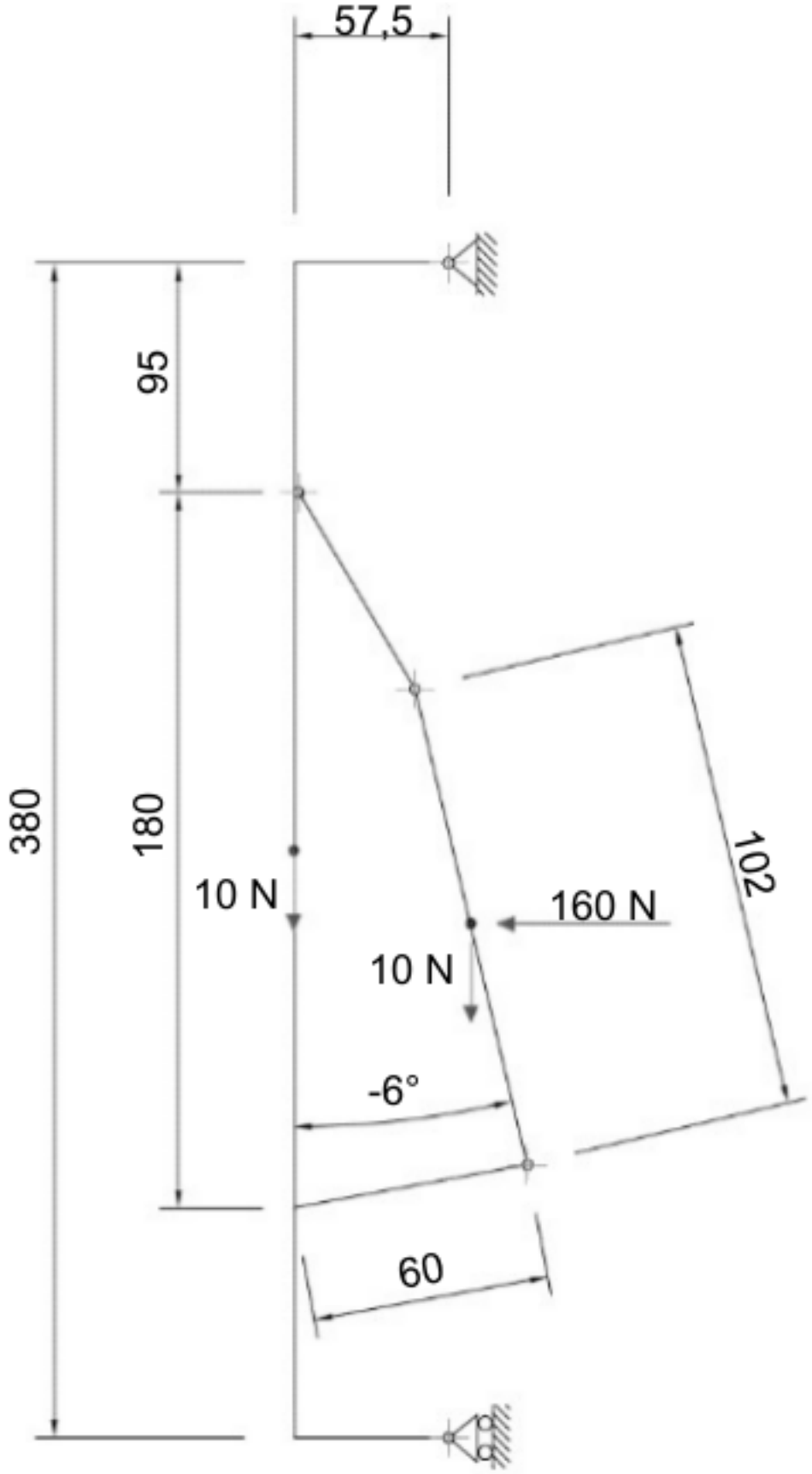

Fig. 18: Figure 2-18 Load configuration for $\theta = 6°$ and $\beta = 90°$

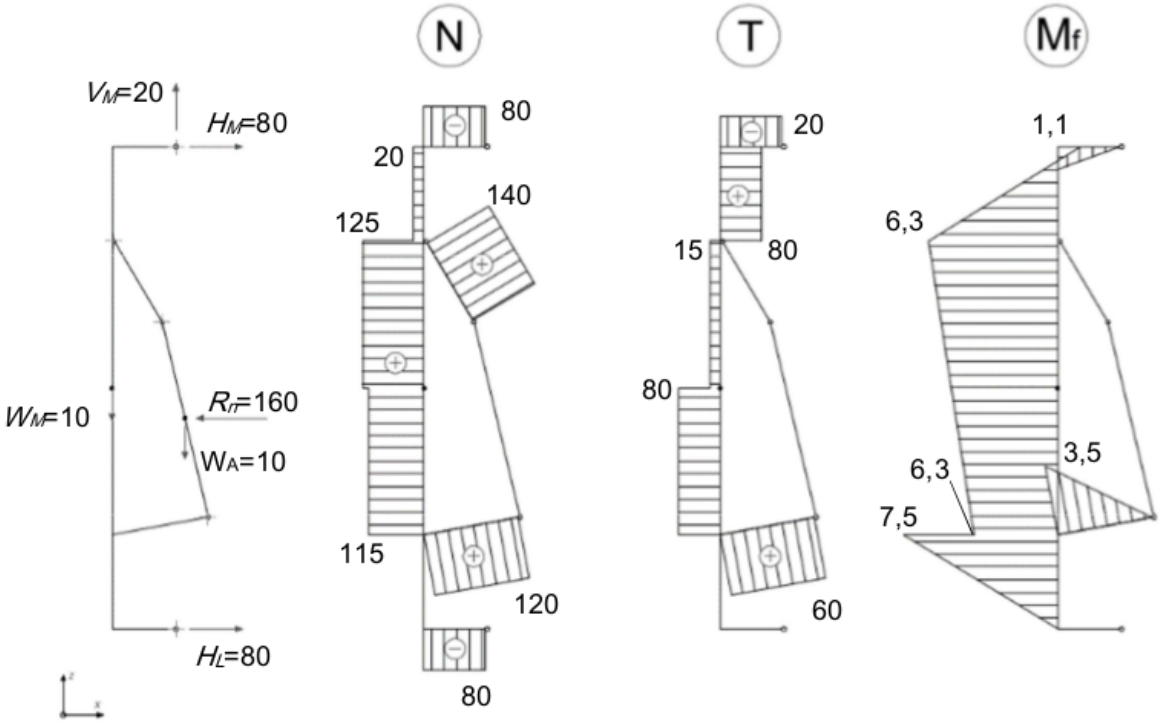

Fig. 19: Figure 2-19 Load chart for $\theta = 6°$ and $\beta = 90°$

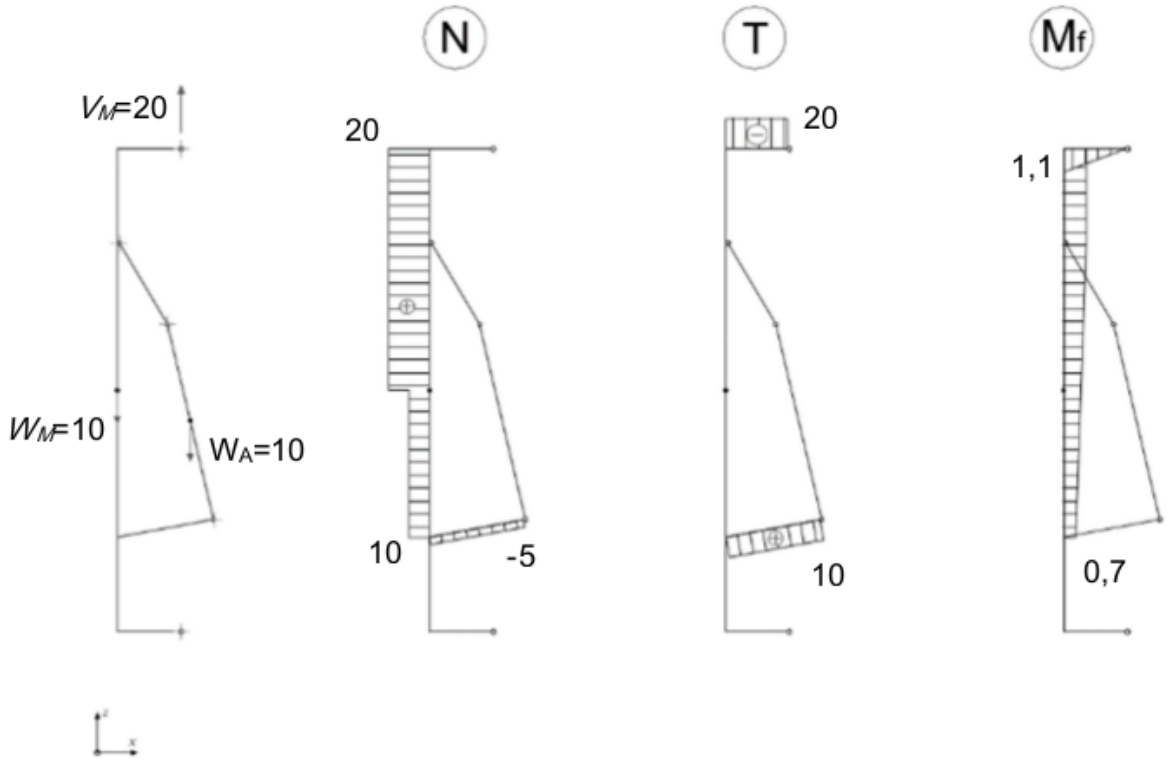

Fig. 20: Figure 2-20 Load chart for $\theta = 6°$ and $\beta = 0$ – effects of weight

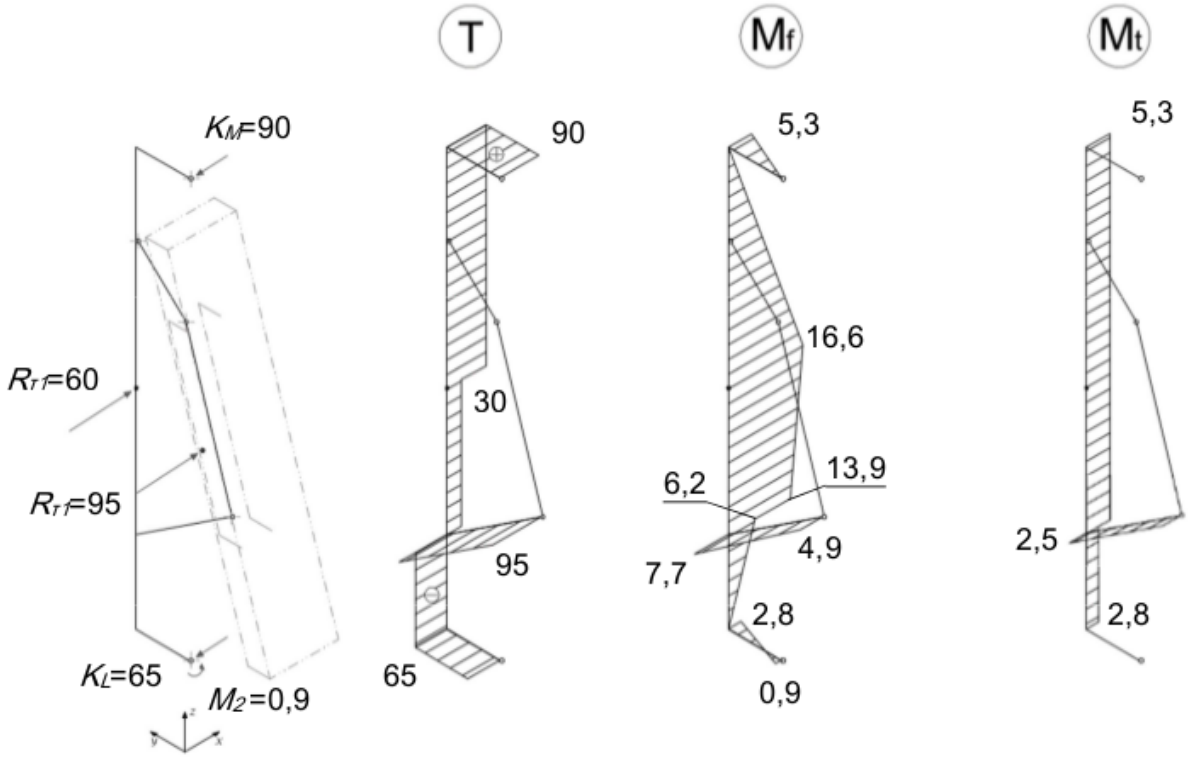

Fig. 21: Figure 2-21 Load chart for $\theta = 6°$ and $\beta = 0$ – effects of side wind

CHAPTER 4

Adopted Solutions

To understand the reasons behind some crucial decisions, it is useful to go through the evolution of the prototype of the Turnantenna. That will be discussed in the first part of this chapter.

In the second part, some characteristic choices will be argued and verified.

4.1 Evolution of the prototype

The actual version of the Turnantenna model is not the first one. During design, a big effort was devoted to figure out a clever concept, able to meet the needs of the final users and to work safely in hard *working conditions*.

4.1.1 Turnantenna V1

The first version of the prototype was strictly intended to define a working electronic system. Electronics was a priority, since the whole system has a very limited power capability.

The Figure 3-1 outlines connections between the electronic components. This setup works and is already in use.

In the image below, it is possible to notice the *ground routing* configuration discussed before. In fact, the router is situated in an accessible place inside the building and while the antenna is outside. The router is the intelligent element and hosts the networking daemon; the antenna works just like a repeater and doesn't take any decision.

The elements in the scheme, following a clockwise order, are:

- a router;
- a POE injector, which supply the 24W of power to the outer components trough the Ethernet cable;
- the Ubiquity NanoStation M5 antenna, that has two Ethernet ports, one for the input and one for the output. The antenna works to 24 volts;
- a splitter to separate data connection from electric power;
- a DC/DC converter that reduce the 24 volts to 5 volts, consistent with the voltage supply of the boards;

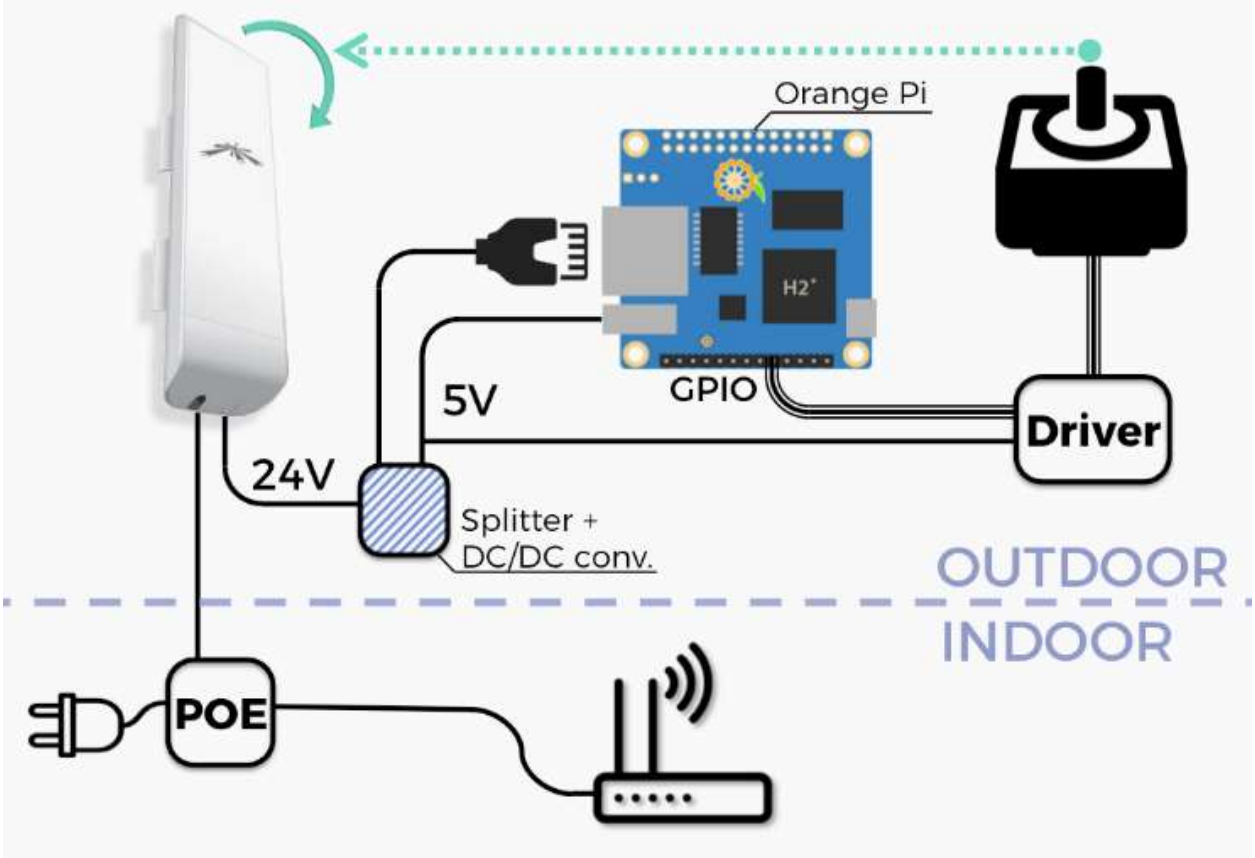

Fig. 1: Figure 3-1 Electronic scheme

- an Orange Pi, a small sized computer. It has all the elements necessary for hosting an operative system (i.e. CPU, HD, RAM), for receiving commands from a network (i.e. network interface), and for controlling the engine drivers (i.e. GPIO pins);
- the drivers and the engines.

The first prototype is shown in the following pictures:

Fig. 2: Figure 3-2 The first version of the prototype of the Turnantenna

4.1.2 Turnantenna V2

Once it has been established that the electronic is working, the next step was to think about a mechanical structure that fully met the *design requirements* .

In this version, the central element remained similar to the older one; a big effort was spent to think at an easy-to-replicate tilt system. It was introduced the four-bar linkage because of its simplicity and the advantages of its use i.e. the mechanical stress induced by the wind is absorbed by the pin of the linkage, and not by the shaft of the engine. This last point is important, since the rotational stresses are very limited compared to the forces on the rockers.

To keep things simple, one of the best solution is 3D printing, used for all the blue pieces in the following renders (Figure 3-3 and Figure 3-4).

FFF printing represents a very cheap solution and allows the realization of very complex parts with minimal difficulty. For example, if in the future the antenna will be substituted, a new set of supports could be printed to adapt the whole structure to the new device.

The plastic used is the ASA (Acrylonitrile Styrene Acrylate), which has a high resistance to the UV and very good mechanical properties. The Table 3-1 Formfutura ApolloX ASA technical data sheet shows the technical data provided

by the vendor.

Property	Typical value	Test Method	Test Condition
Specific gravity	1100 kg/m^3	ISO 1183	
Tensile strength	47,5 MPa	ISO 527	@ Yield 50mm/min
Tensile modulus	2020 MPa	ISO 527	1 mm/min
Melting temperature	$\pm$ 230 $\pm$ 10°C	ISO 294	
Viscat softening temp.	$\pm$ 98°C	ISO 306	VST/A/50 (50°C/h, 10N)

Table 3-1 Formfutura ApolloX ASA technical data sheet[1]

As can be easily seen in Figure 3-4, the kinematic chains are formed by the engine and a gear reducer (enclosed inside the blue ASA carter), the synchronous pulley and belt system. The reason why all these reduction steps are needed is that engines are very small, due to the very limited electrical power available, and the wind action is remarkable. More details on the *engines* design will be provided later.

Another detail that should be noted is the use of rod end bearings for the upper rocker. Using this particular joints, the structure gains more construction error tolerance, and is not subject to the risk of binding.

4.1.3 Turnantenna V3

During the realization of the real prototype, the first problem encountered was the weight of the main piece of the moving frame. This piece is made of a tube and a flanged pin, welded together.

The intrinsic problem of this solution, for a non-professional mechanic, is that it requires the usage of steel. Steel is the cheapest, easy to weld, easy to find metal. Since the primary target of this work are low-skill people, steel is the only solution. But steel is very heavy, and the piece mentioned earlier reached the weight of more than 1 kg. One alternative solution is the usage of aluminium, which is not easy to weld, and requires specific, more complex and costly welding machines.

In addition to the weight, another problem comes from the realization of the turned pin: it requires a lathe.

[1] Formfutura VOF, "Technical Data sheet, Product name: ApolloX, Date of issue: 22 April 2016, Version: v1", www.formfutura.com

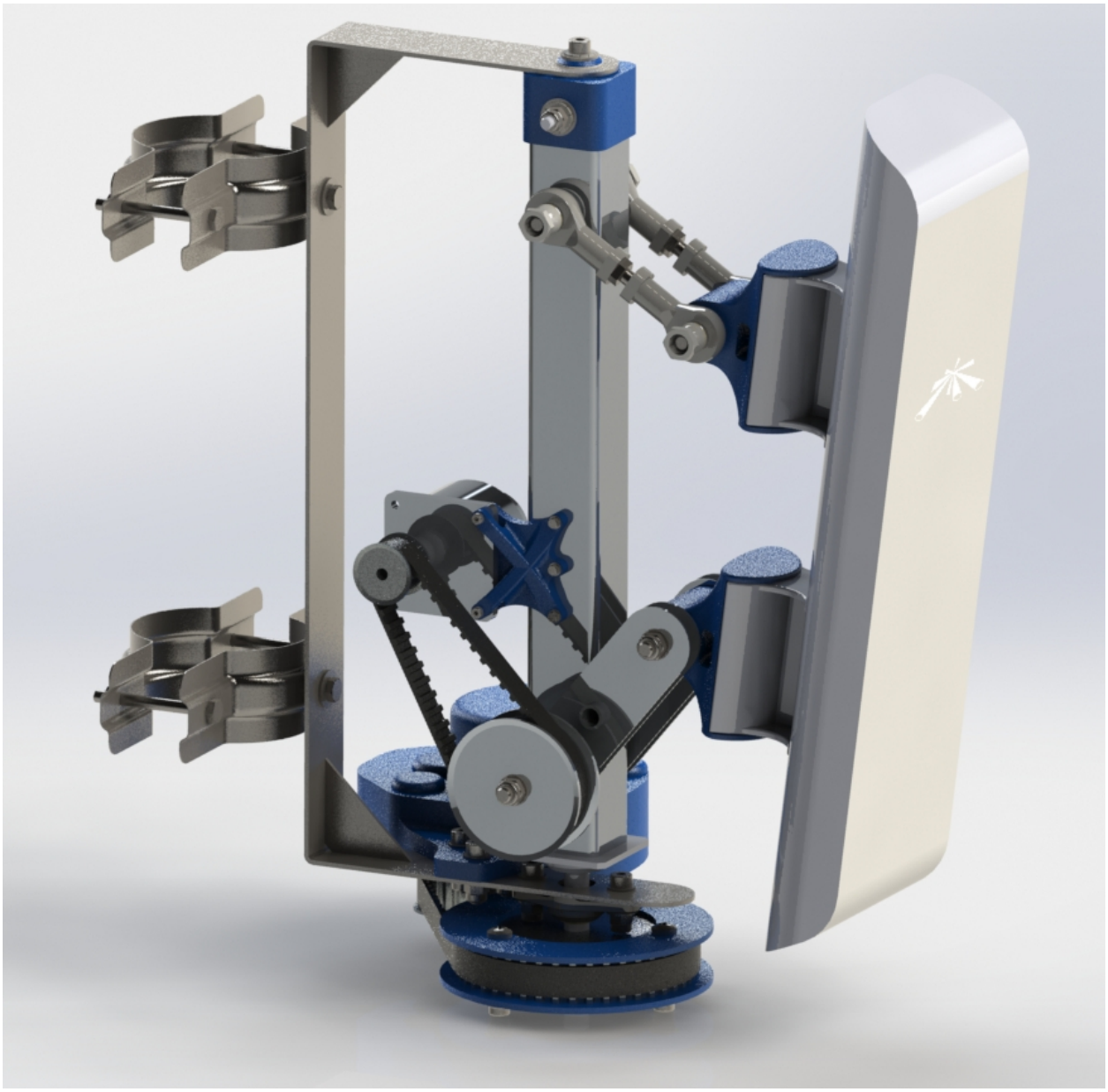

Fig. 3: Figure 3-3 The second version of the prototype of the Turnantenna

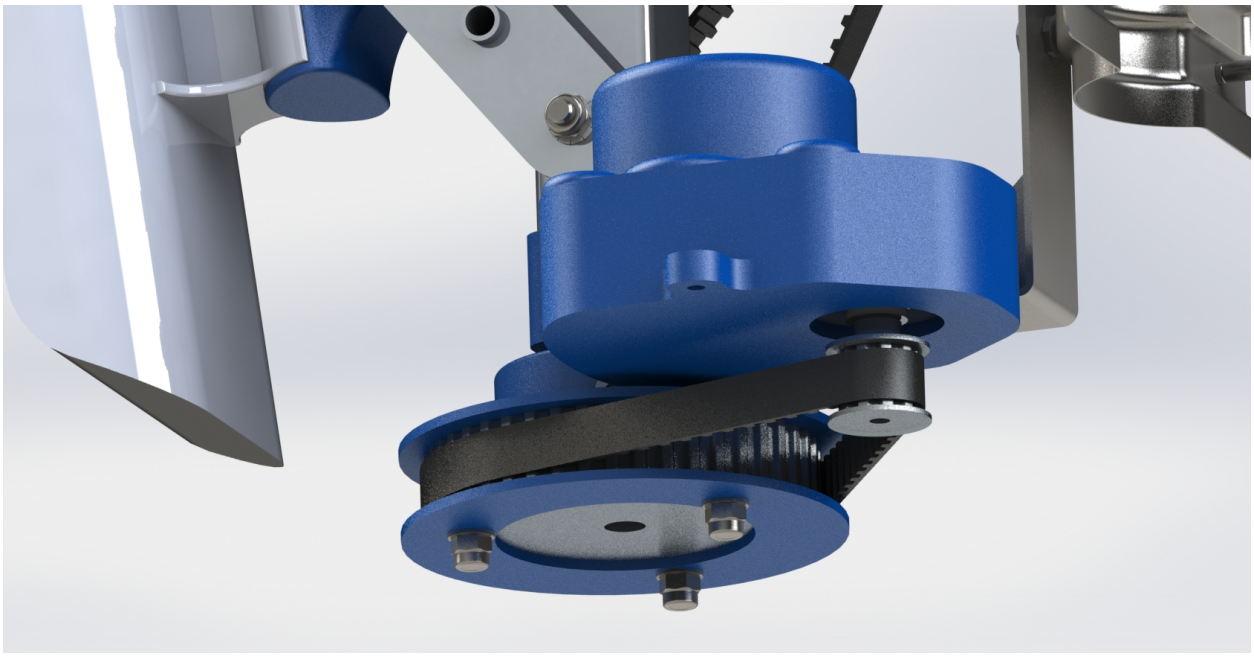

Fig. 4: Figure 3-4 The lower kinematic chain

Figure 3-5 The central piece of the mobile frame in Turnantenna v2: the pin, the tube and the assembled component

For all the reasons listed above, in the newer version the straight steel tube was replaced with a C shaped aluminium one. This change brought some other side benefits:

- the connection between the mobile frame with the fixed one has become easier
- the torque exerted on the second engine was decreased of about one order of magnitude

Figure 3-6 and Figure 3-7 show the more practical mounting system in the newer version.

In Figure 3-6, (1) is the flanged pin; (2) is a flange bearing; (3) is a pulley; (4) is a plastic cap, which has a nut embedded; (5) is the fixed frame; (6) is a thrust washer. The cap is fastened with the central element of the mobile frame; the top bolt assure a spacer with the cap, leaving a little clearance between the frame and the lower surface of the spacer. Thanks to this gap, the thrust washer allows the rotation of the mobile frame, which is controlled by the pulley, force matched with the pin.

In Figure 3-7, (1) is a bolt; (2) and (4) are tubes; (3) are thrust washers; (5) is a flange bearing. The bolt fastens the tube and the mobile frame together; the tube is a bit longer than the fixed frame thickness, and leave a clearance where to place the thrust washers. In the bottom, another bolt keeps the tube (4), and another tube below, fixed together with the mobile frame; the frame will rotate under the action of the engine (not shown) on the bolt.

Figure 3-8 shows the difference in the torque between the two versions, caused by a change in the distances between the application point of the wind forces and the axis of rotation.

This kind of reduction in the C_2 magnitude allows the removal of the belt reduction system, reflecting on a lower weight of the entire system, a considerable cut of the cost and a simpler setup operation.

Another changes have been done to make the system simpler and stiffer, i.e.:

- the lower rocker was designed to be 3D printed, since the older version was unnecessarily complex;
- the main frame is now made of rectangular section welded tubings, instead of the old cut and bended sheet. In this way the system results to be stiffer.

4.2 Components selection and verifications

The Turnantenna project is not close and the optimization work is in progress. The list of requisites that guides the designing process could be found *here*; solutions can be verified using the equations *here* and, in the end, their application are tested on the prototype.

In this section the most important solutions will be discussed.

4.2.1 Polymer bearings

Polymer bearings have several advantages: they are

- self-lubricant
- compact
- resistant to dust, dirt and water
- cheap

Polymer bearings resist in a relative wide temperature range, from -40°C up to 130°C for long-term applications.

In the Turnantenna system, polymer bearings are a very good solution since they are cheap, easy to use and there is no need to do maintenance.

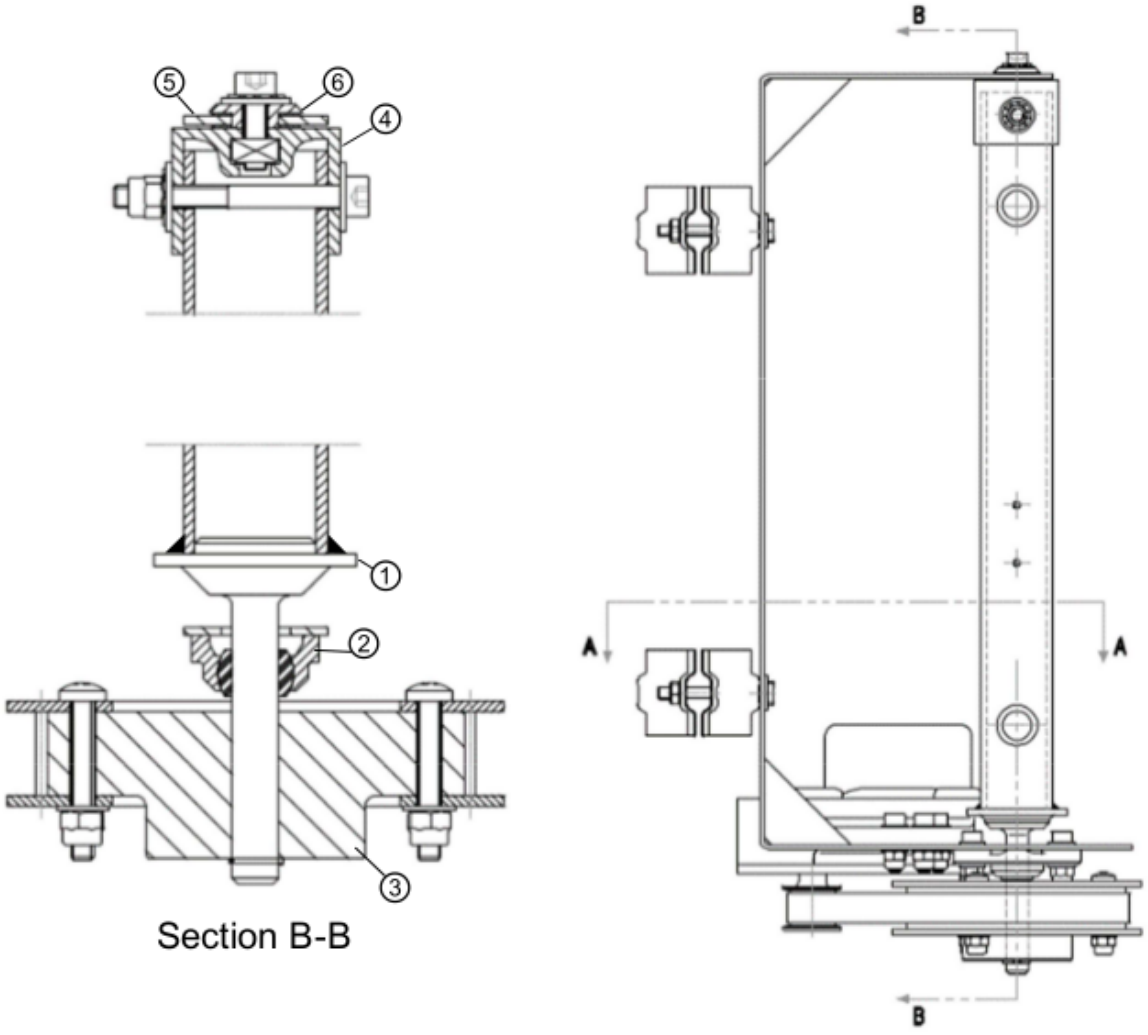

Fig. 5: Figure 3-6 Turnantenna v2 connection system

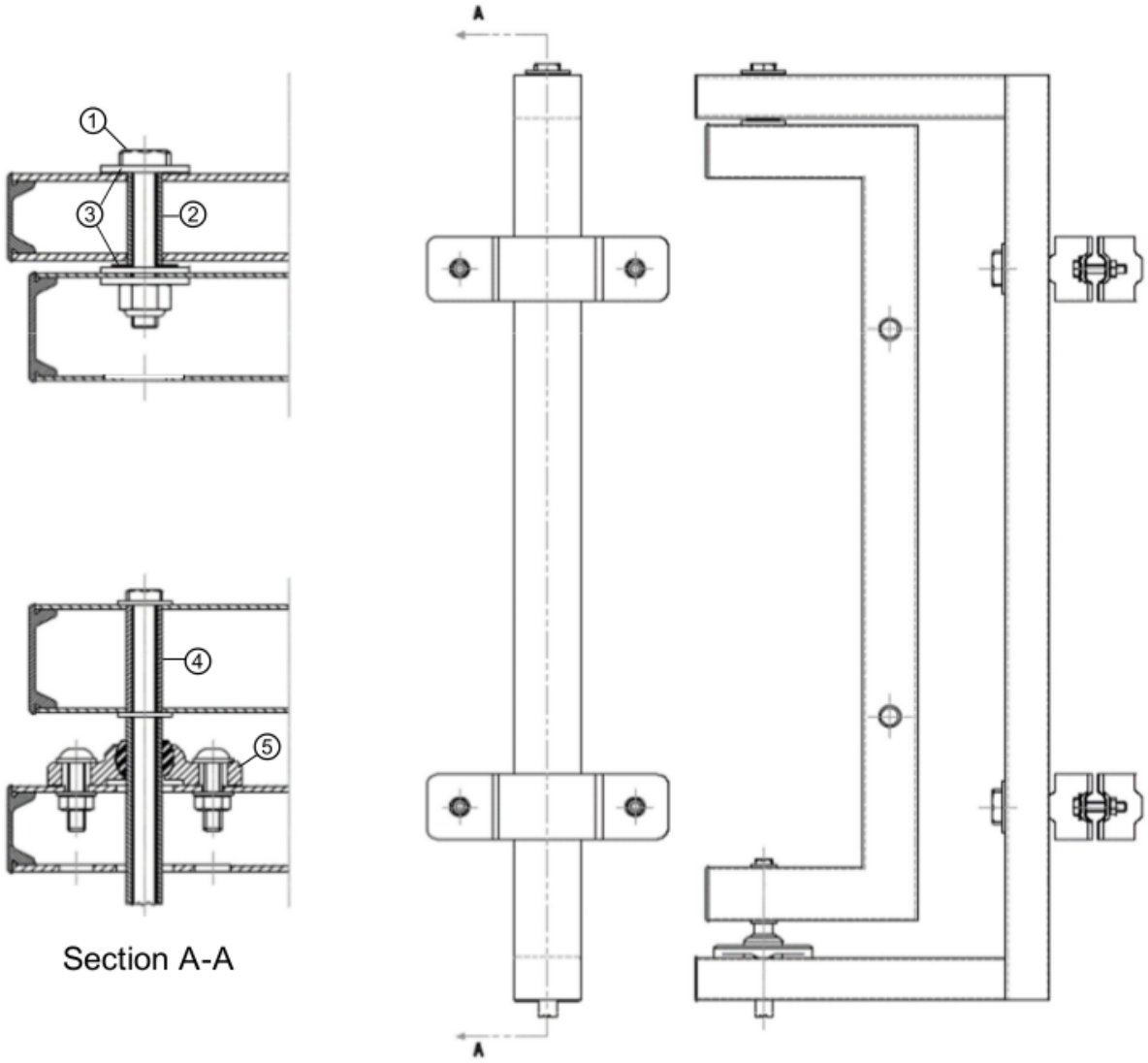

Fig. 6: Figure 3-7 Turnantenna v3 connection system

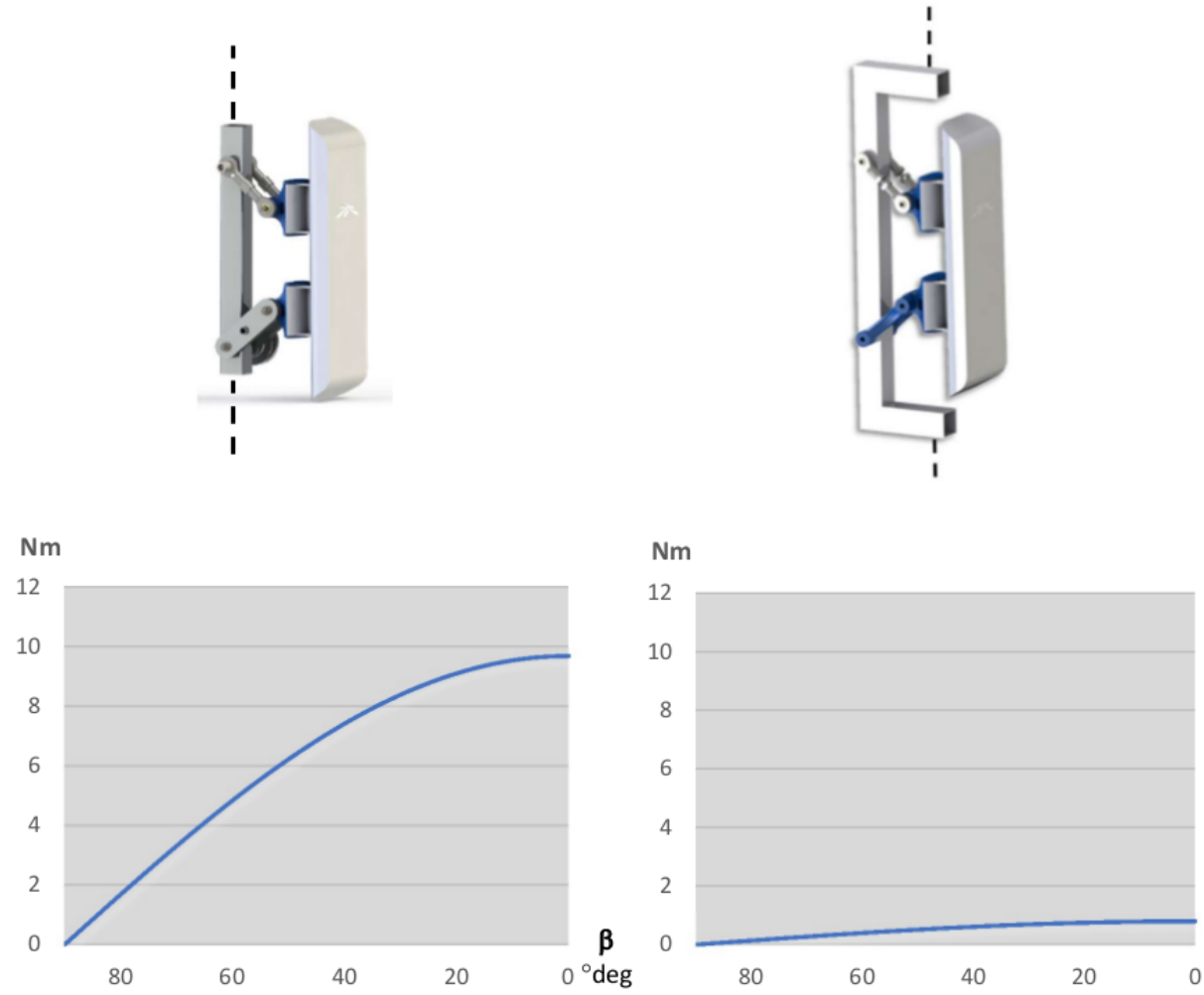

Fig. 7: Figure 3-8 Difference of C_2 torque between Turnantenna v2 (left) and v3 (right)

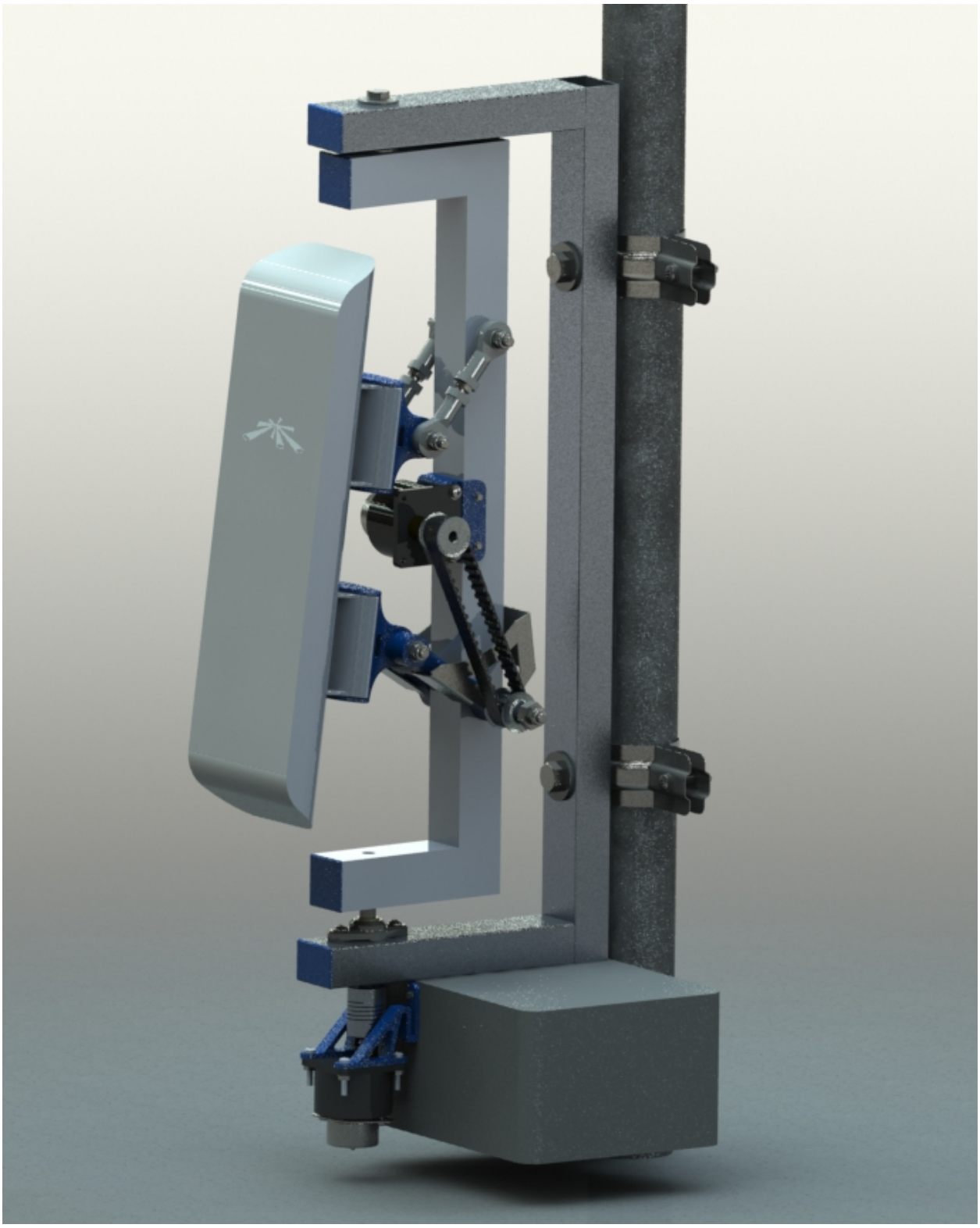

Fig. 8: Figure 3-9 The third version of the prototype of the Turnantenna

Thrust washers

Polymer thrust washers permit the turning of the mobile frame, in presence of compressive forces, dust, dirt and high humidity.

They are positioned in the top pin, between the washers and the fixed frame. The bolt tighten the washers, the tube and the mobile frame together, while the bearings are free to float, held in place by gravity. The upper bearing sustain the weight of the mobile assembly, the lower one is there for safety, to provide support in rare cases of updrafts.

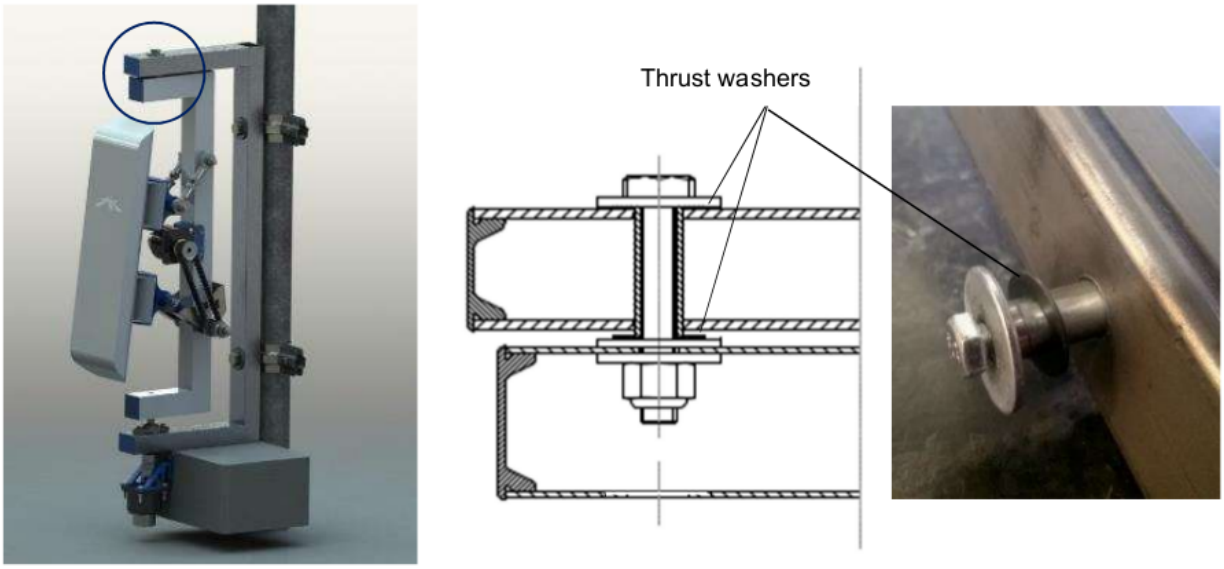

Fig. 9: Figure 3-10 Polymer thrust washers position

The upper washer is under the *compressive effect of the force* $V_M = 20\ N$. The component used is the iglide G300 GTM-0815-005 by igus, which has the following characteristics:

Property	Typical value	Test Method	Tolerance
Shaft diameter	8,0 mm	•	+0,25 mm
Outer diameter	15,0 mm	•	-0,25 mm
Thickness	0,5 mm	•	-0,05 mm
Pv value, max. (dry)	0,42 MPa·m/s	•	•
Max. recommended surface P	80 MPa	•	•
Max. long-term application T	130 °C	•	•
Low application T	-40 °C	•	•

Table 3-2 igus iglide G300 GTM-0815-005 technical data sheet

The pressure applied on the bearing, and the average linear speed are:

$$P = \frac{4F}{\pi(D^2 - d^2)} = 0,16\ MPa$$
$$v = \omega \cdot \overline{r} \approx 0,1\ m/s$$

assuming a rotation speed in the order of magnitude of 1 rad/s (it is an ideal maximum, in reality it will be slower). The resulting values are very small and, putting them inside the charts below, they result to be perfectly verified for every reasonable working conditions.

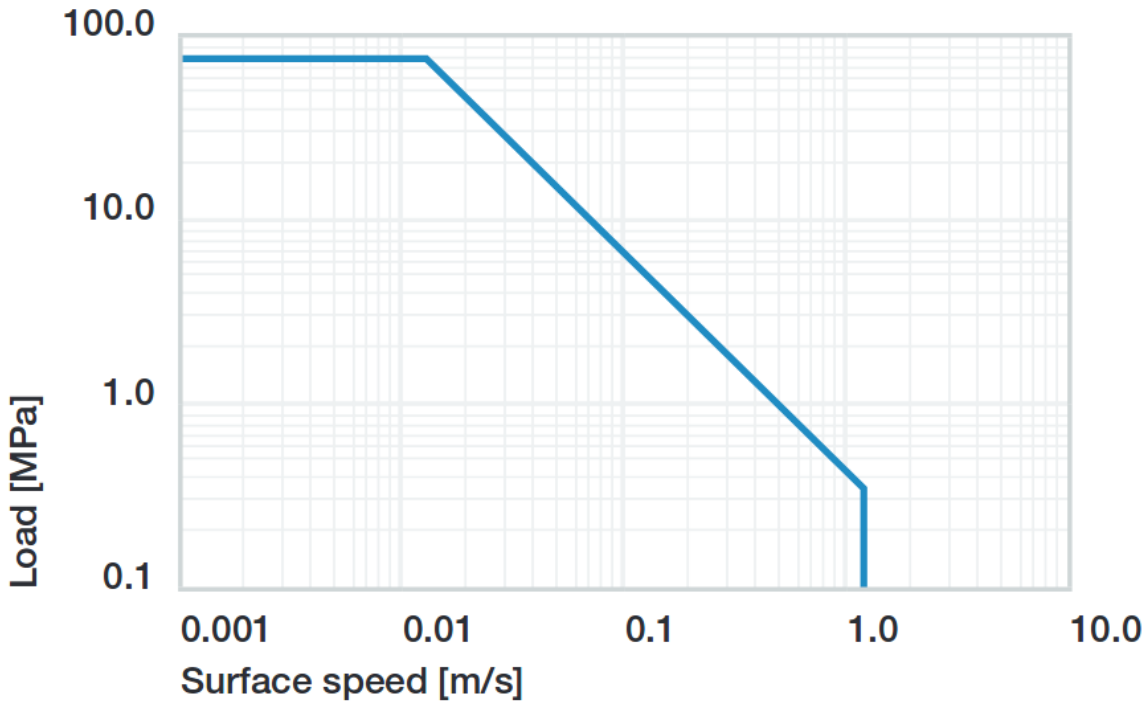

Fig. 10: Figure 3-11 Permissible Pv values for iglide G with a wall thickness of 1mm in dry operation at 20°C

Sleeve bearings with flange

This kind of bearings are used for all the four-bar linkage pins. Pins are made of threated rod M5. The force exerted on the pin is diffused by a tube with the internal diameter of 5 mm, which also works as spacer between the rockers.

The safety nuts are tightened on to the rockers, kept in position by the tube. Sleeve bearings are assembled on the central piece (the antenna support in Figure 3-13) with interference. The whole width of the central element is a bit shorter than the tube. In this manner, when rockers are fastened together with the tube, the central element can freely rotate on it, because no pressure is exerted on its sides.

Washers help to diffuse the pressure between the elements.

As seen *before*, the most critical element is the beam 3 when β = 0 and θ = 6°. In this situation, the pin between the lower rocker and the mobile frame is under the combined effect of the following forces:

- $T = 10\ N$
- $N = 5\ N$
- $M_f = 4,9\ Nm$
- $M_t = 2,1\ Nm$

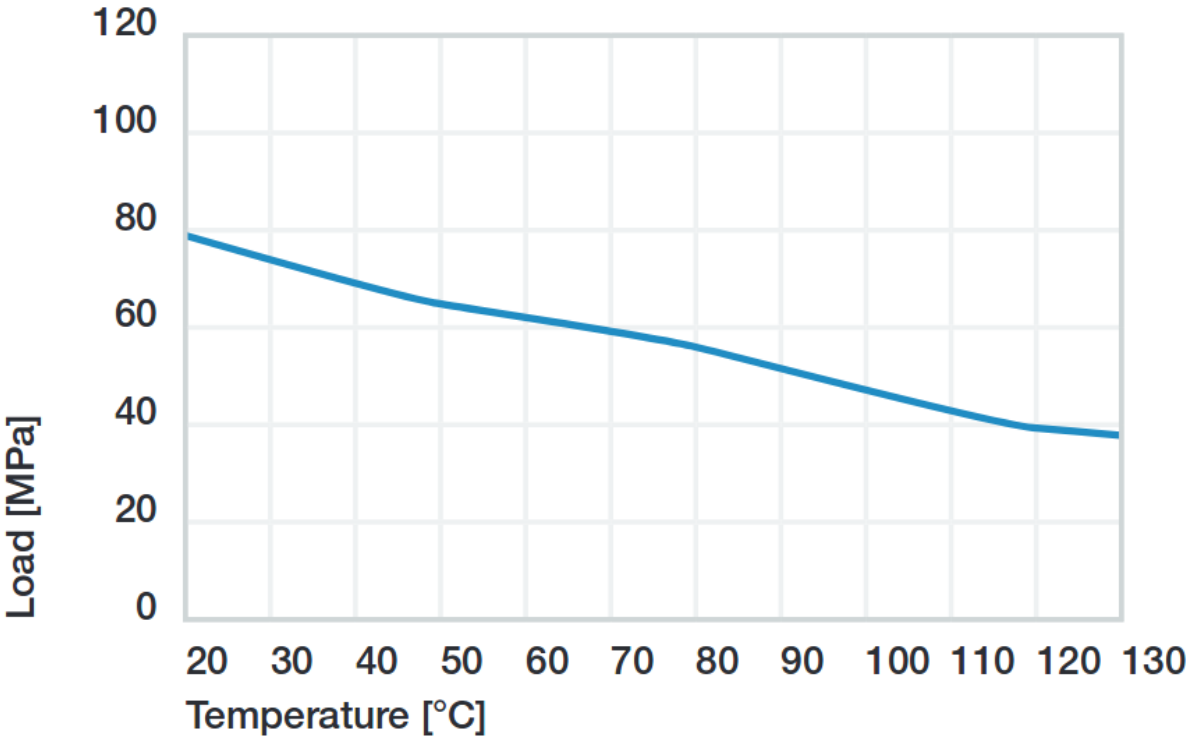

Fig. 11: Figure 3-12 Recommended maximum surface pressure as a function of temperature (80MPa at 20°C)

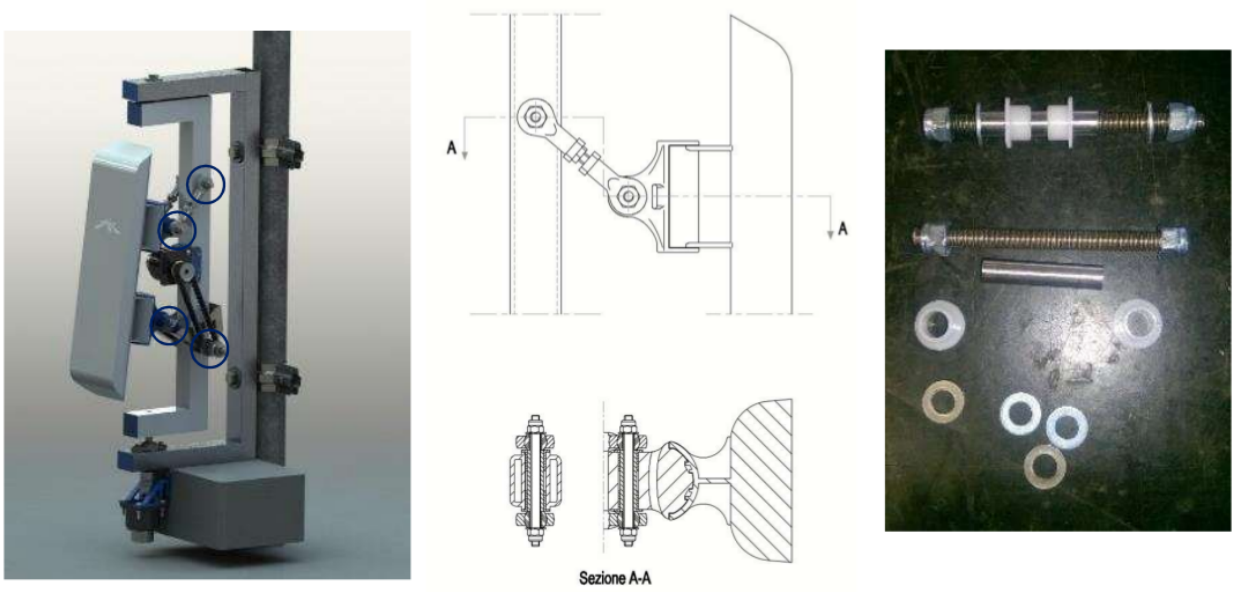

Fig. 12: Figure 3-13 Polymer sleeve bearing positions

Considering forces exerted by the wind on the beam 3, they have the directions represented in Figure 3-14. T and M_t have the same direction of the rocker (δ angle), N and M_f are perpendicular to it.

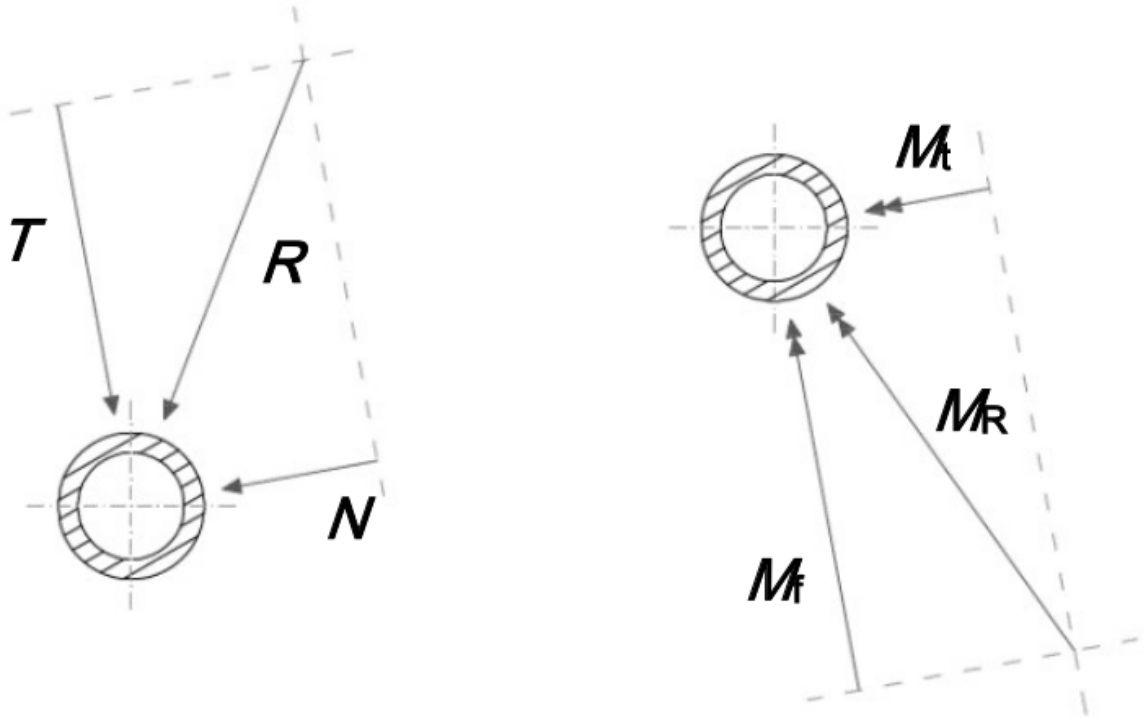

Fig. 13: Figure 3-14 Force analysis on sleeve bearings

In Figure 3-15 there is the scheme adopted to evaluate the effect of the forces on the bearings: a force, or moment, can be deemed equivalent to a pressure applied on to the contact surface. To simplify, pressures are considered uniforms. Therefore, a local resultant force acting in the middle is equivalent to those pressures.

Bearings position is defined by the central element, which has a width of 28 mm, and correspond to the distance between the inwards surfaces of the flanges. Sleeve bearings are 5 mm long. The distance between the application points of the forces is:

$$L = \frac{l}{2} + w + \frac{l}{2} = 33\ mm$$

now F_1' and F_2' can be found with:

$$F_1' = F_2' = \frac{M}{L}$$

forces that compose M_t act in the same direction of T ; N is related to M_f instead. R_1 and R_2 are the resulting forces in the two directions:

$$R_1 = T \pm \frac{M_t}{L} = 10\ N \pm \frac{2500\ Nmm}{33mm}$$
$$R_2 = N \pm \frac{M_f}{L} = 5\ N \pm \frac{7700\ Nmm}{33mm}$$

The $\pm$ symbol represent the fact that one bearing will be stressed by the combination of the two effects, while the other bearing (the parallel one located on the same axis) will bear the difference between the effects.

R_1 and R_2 are mutually perpendicular and, in the worst case, their sum is:

$$R_{tot} = \sqrt{R_1^2 + R_2^2} = 253\ N$$

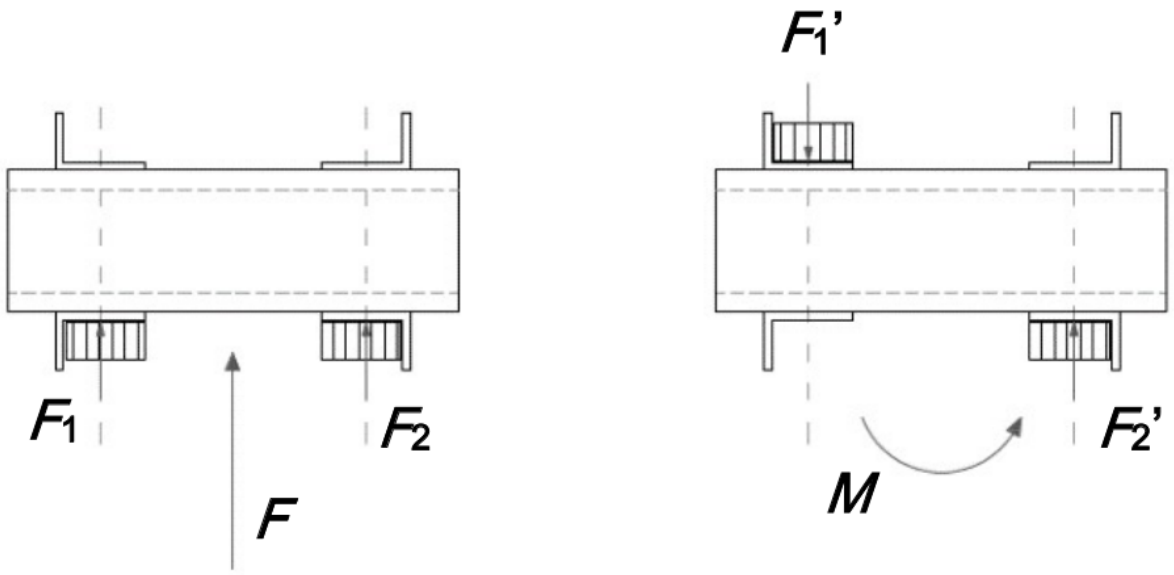

Fig. 14: Figure 3-15 Force analysis on sleeve bearings

Since the bearing inner diameter is 6mm, and it length was specified above:

$$P = \frac{R_{tot}}{l \cdot d} = 8,4\ MPa$$

The bearing chosen is the iglidur R A180, and the following table summarise its characteristics:

Property	Typical value	Test Method	Tolerance
Shaft diameter	6,0 mm	•	E10
Outer diameter	8,0 mm	•	H7
Thickness	1 mm	•	•
Pv value, max. (dry)	0,31 MPa·m/s	•	•
Max. recommended surface P	28 MPa	•	•
Max. long-term application T	90 °C	•	•
Low application T	-50 °C	•	•

Table 3-3 igus iglide A180 A180FM-0608-06 technical data sheet

The low pressure and the speed comparable with the one calculated for the thrust washers in the previous section, guarantee the good working conditions of the sleeve bearings with flange in all the reasonable conditions considered in this work.

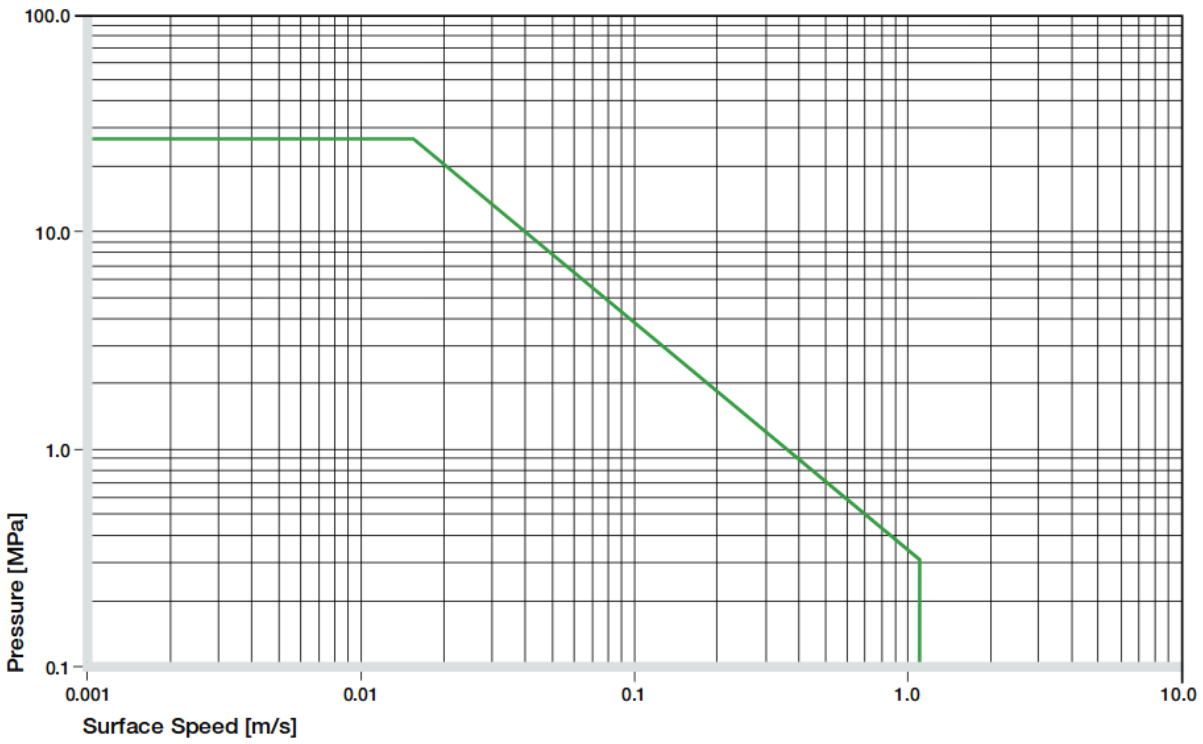

Fig. 15: Figure 3-16 Permissible Pv values for iglide A180 with a wall thickness of 1mm in dry operation at 20°C

Articulated heads

The upper rockers of the four-bar linkage are made of two of those particular elements, jointed together by a piece of threated rod M5 (Figure 3-18). The assembly of the articulated heads with the pin is shown in Figure 3-13; in this case, the threated pin is in direct contact with the metal sleeve of the rod end.

Articulated heads have been chosen to avoid the binding of the system. According with the hypothesis that the Turnantenna could be built by unexperienced people, the probability of make machining errors is very high. If all the four linkage axis are not perfectly aligned, the system do not work properly. The adoption of spherical joints, instead, provides a high error tolerance.

According to the stress analysis, on these components is applied just one force: it is parallel to the rocker direction, and its magnitude is pair to 140N when $\theta = 6°$ and $\beta = 90°$ (frontal wind). This means that the resulting force exerted on a single head is 70N.

The articulated head has the following characteristics:

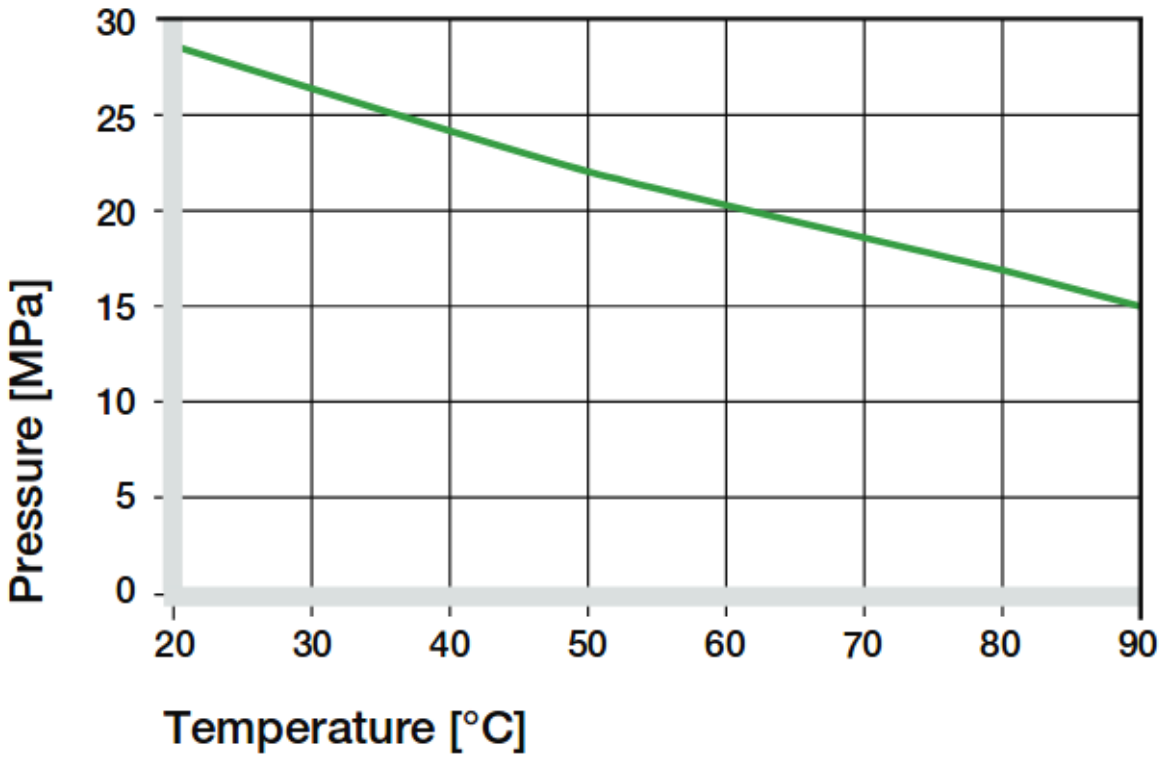

Fig. 16: Figure 3-17 Recommended maximum surface pressure as a function of temperature (28MPa at 20°C)

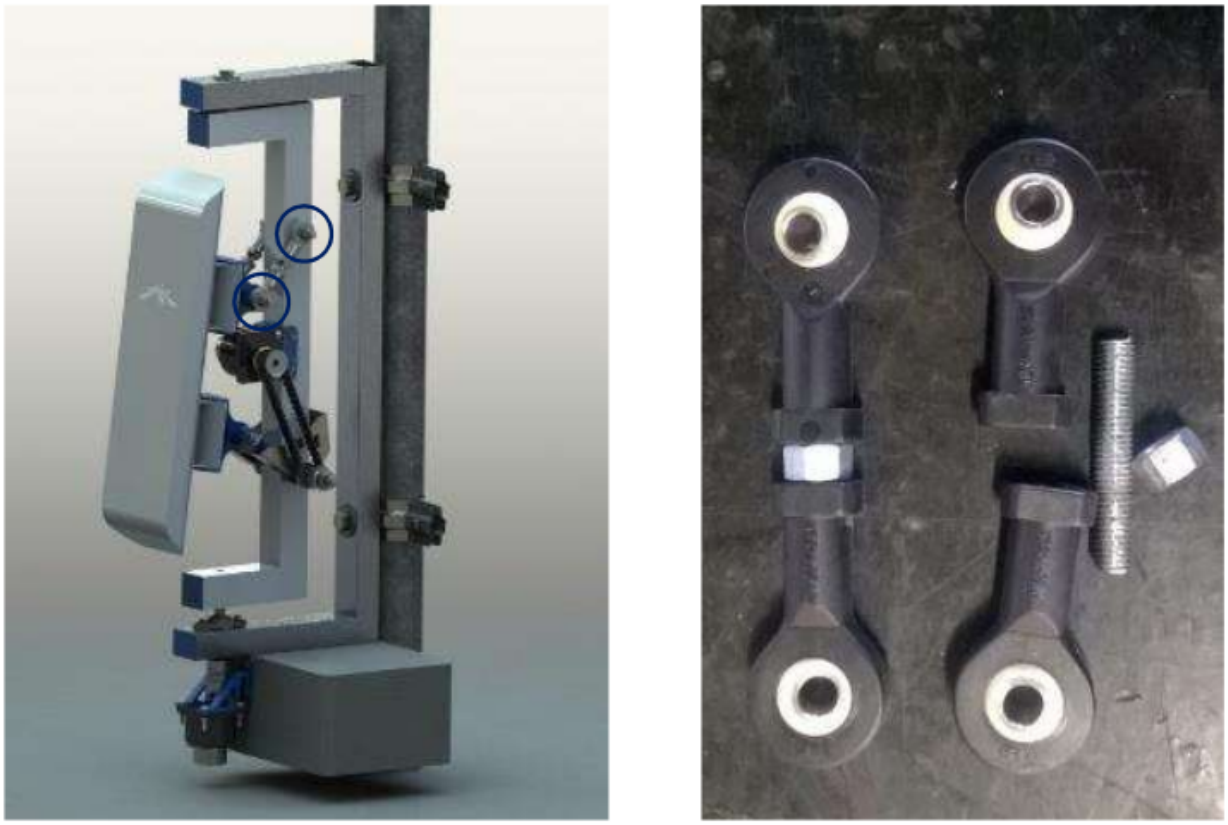

Fig. 17: Figure 3-18 Picture and render

Property	Typical value	Test Method	Tolerance
Shaft diameter	5,0 mm	•	•
Thread	M5	•	•
Max pivot angle	30°	•	•
Max. static tensile strength	500 N	•	•
Max. radial load	125 N	•	•
Max. torque strength through ball	12 Nm	•	•

Table 3-4 igus igubal KBRM-05 MH technical data sheet

In all the cases, the force exerted is low enough to make the system work with a high safe margin.

Flange bearings

The upper revolute joint of the mobile frame is made with a pin and two thrust washers. The lower joint, instead, is a flange bearing, and this choice has been done for many reasons:

- it keeps the structure isostatic
- it amplifies construction and machining errors tolerance, also thanks to the oblong holes
- helps during assembly: one time the lower pin and the central body of the mobile frame are mounted together, they can tilt; the insertion and the extraction of the element in place become much more easier and do not require the disassembly of the component

The flange pin is showed in the next figure. The section is extracted from Figure 3-7

The worst case scenario for this component is when the wind blows from the front. In that situation, it has to bear a horizontal force of 80N.

Property	Typical value	Test Method	Tolerance
Shaft diameter	8,0 mm	•	•
Length	44,2 mm	•	•
Oblong hole d x l	4,3 x 6,5 mm	•	•
Max pivot angle	25°	•	•
Max. permitted axial load	350 N	•	•
Max. permitted radial load	550 N	•	•

Table 3-5 igus igubal EFOM-08 technical data sheet

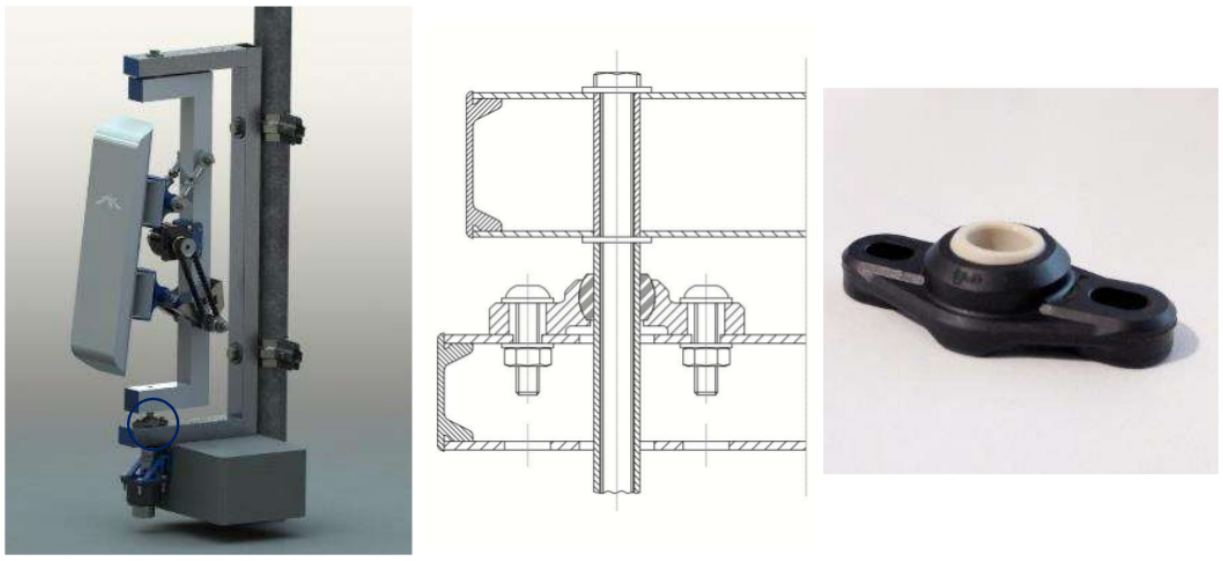

Fig. 18: Figure 3-19 Flange bearing position

Again, the maximum load permitted long term is a grade of magnitude higher than the maximum force, and the EFOM-06 could be enough. The EFOM-06 is smaller, and its shaft diameter is 5mm, perfect to fit with a M5 rod end, like the previous bearings. EFOM-08 needs a new rod instead, and this choice is not the best, from a practical point of view.

4.2.2 Stepper Engines

The choice of how to move the Turnantenna was not so simple. The market offer a wide range of engines, of different types, but stepper motors was rated as the best choice.

Stepper engines has a bad electrical efficiency, but are accurate in the movement, since they move one step at time; they are brushless and have a long lifetime. But the key advantage of those motors is a consequence of the permanent magnets they have inside. Even when the engine is not powered, there is a residual torque exerted by the engine. The implications of this characteristic will be clear next.

To summarise what wrote before, the engines have to respect the following conditions:

- the overall power consumption for both the engines must be lower than 7W
- max torque exerted by the wind are $C_1 = 3,5\ Nm$ for the horizontal axis, and $C_2 = 0,9\ Nm$ for the vertical axis.

Engines

The limited power source do not allow to use one engine alone. A reducer is needed to amplify the small torque and bear the wind load.

The engine of choice, for both the cases, is the McLennan 26M048B-1U, which has the following characteristics:

Property	Typical value	Test Method	Tolerance
Typology	Unipolar	•	•
Holding torque (engine stationary)	0,009 Nm	•	•
Tension	5 V	•	•
Current	250 mA	•	•
Step angle	7,5°	•	•
Steps per revolution	48	•	•

Table 3-6 McLennan 26M048B-1U technical data sheet[2]

The power consumption is approximately the twice the product between voltage and tension (because there are two coils powered at a time), that results to be 2,5 W per motor. Two of those engines leave enough energy to manage possible power peaks, and to expand the Turnantenna with some other device (e.g. passive sensors, other kind of antennas like radio or LoRa, ecc.).

The torque exerted by the engine changes with the speed of rotation. The operation diagram below shows how the motor behaves in a range of different rotational speeds.

where 1 PPS (Pulse per Second) is equivalent to 60s/48steps = 1,25 rpm.

Having the characteristics of the engines, the next step will be choosing the gear reducers.

Reducer 1

The first reducer is one of the most critical elements of the entire Turnantenna system. To provide a correct torque at the end of the kinematic chain, the reduction ratio has to be more than

$$\tau = \frac{3,5\ Nm}{0,009\ Nm} = 389$$

In addition to this, the reducer will obviously bear the external torque without breaking and, hopefully, in case of overload, it has to be sufficiently tough to resist and allow the loss of step by the engine.

A reducer that satisfy all these requirements is the Crouzet 81037005, which has the following characteristics:

Property	Typical value	Test Method	Tolerance
Output ratio	500:1	•	•
Max torque	5 Nm	•	•

Table 3-7 Crouzet 81037005 technical data sheet

When the wind blows at the maximum speed (37,5 m/s), the resulting torque of the gear reducer will be:

$$T = 0,009 \cdot 500 = 4,5\ Nm > C_1 = 3,5\ Nm$$

[2] igus, 2018, shop online: www.igus.com

Fig. 19: Figure 3-20 McLennan 26M048B-1U

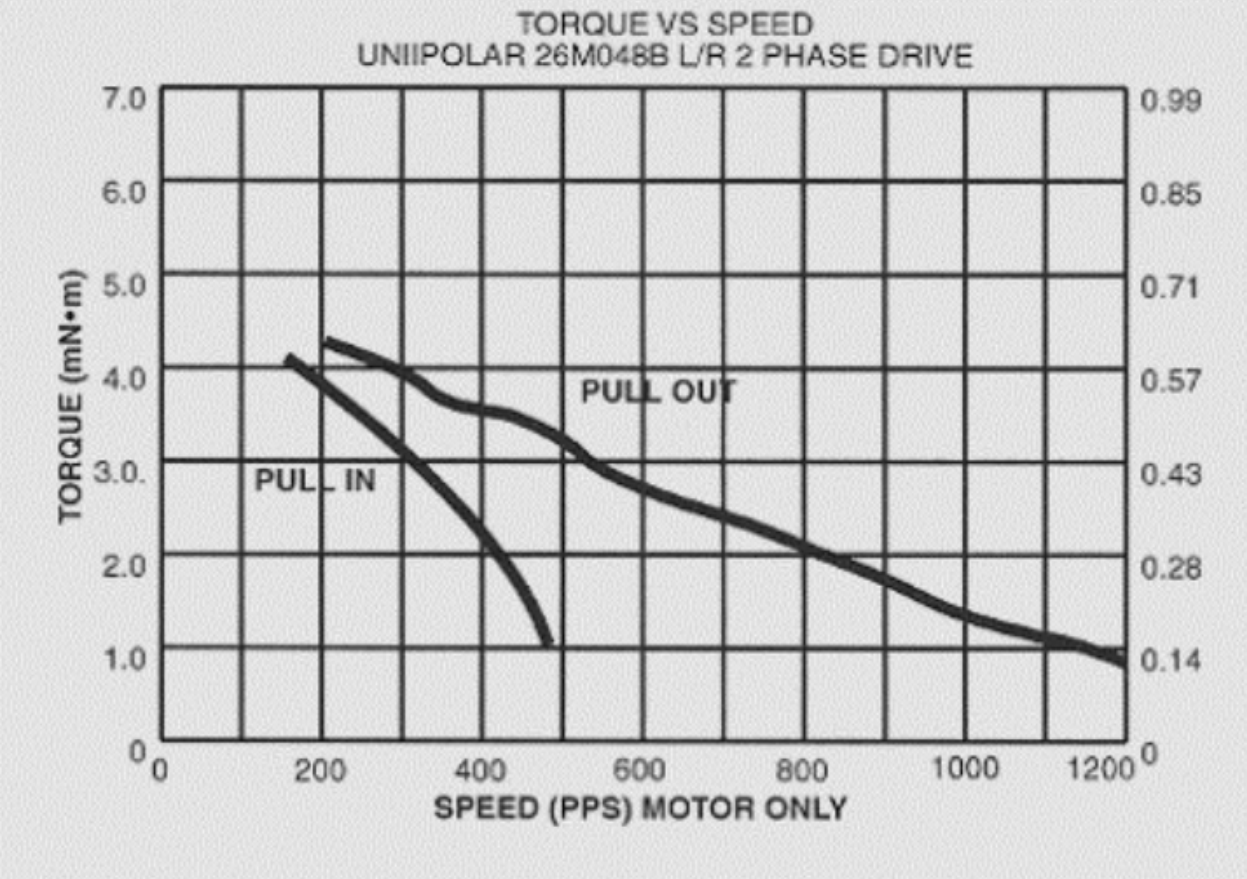

Fig. 20: Figure 3-21 Operation diagram of McLennan 26M048B-1U

This value is enough to keep the antenna in position. Moreover, if a gust of wind overloads the antenna, exerting a torque greater than 3,5 Nm, the engine will lose steps, and lose the orientation, but the gear reducer will be safe and will not burst.

The only problem of this reducer, is its cost that is excessive related to the rest of the system. This is why in future a different system will be studied to optimise the costs and the performances.

The engine is mounted on the reducer, which is fixed to the mobile frame through a 3D printed bracket. The torque is transmitted by a synchronous belt to the lower rocker.

Reducer 2

The second engine is far less problematic than the first one. The change of the shape from the version 2 to the 3 overturned the situation for this component (see *Turnantenna V3*).

The minimum ratio value is

$$\tau = \frac{0,9\ Nm}{0,009\ Nm} = 100$$

The choice is between two reducers which cost the same, but different ratios. One has 100, the second 200. Since the rotational speed is not important in this case, the choice has gone to the second one because, at the same price, the maximum torque is doubled and a certain safe margin helps in case of future upgrades.

Property	Typical value	Test Method	Tolerance
Output ratio	200:1	•	•
Max torque	1,8 Nm	•	•

Table 3-8 Trident Engineering GS38.0200 technical data sheet

$$T = 0,009 \cdot 200 = 1,8\ Nm > C_2 = 0,9\ Nm$$

that is equal to the construction limit. It is not positive at all, since the reducer may be damaged. The best solution would be to have a gear ratio in the middle between 100 and 200. However, if the torque reaches this value, the wind must blows much faster than the worst cases considered in this work.

The second gear motor is mounted below the frame, fixed to the electronic box. To make the engine works correctly, it needs to be perfectly aligned with the axis of rotation but, since a number of construction errors are possible during the process, a few tricky solutions were needed.

The fixed frame (1) host the electronic box (2), which supports the engine assembly (5)+(6) through its brackets (3). These last are 3D printed with ASA, a flexible plastic, in order to absorb inflections and small displacements of the motor due to a misalignment of the axis, and are mounted with two self-drilling screws. The axial joint (7) tolerate parallelism errors between axes, and connect the gear reducer shaft with the threated rod (8) with two elastic pins. The spacer (9) fix the distance between the top of the joint and the bottom of the mobile frame; it is a tube with the same diameter of the flange bearing (10). On top, the rod is tightened by a prevailing torque nut (11).

** Notes **

The big advantage of having a motor with a residual torque, like steppers, become clear when so reducers have this kind of indexes. A one thousand Nm torque on the engine shaft becomes few tenths on the antenna. There are a lot of situations where the engine can bear the wind force, without being powered ON.

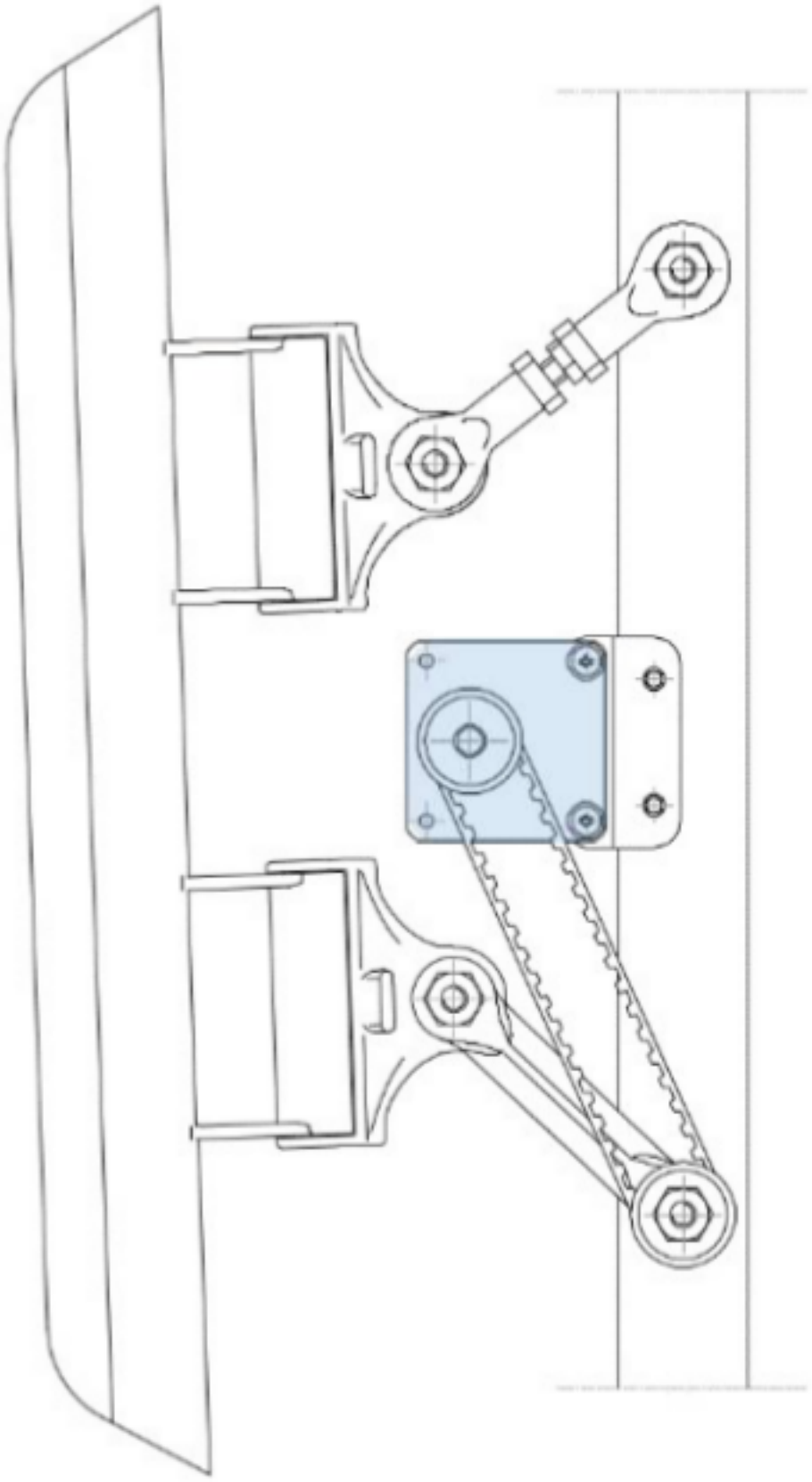

Fig. 21: Figure 3-22 Engine and first reducer mounting representation

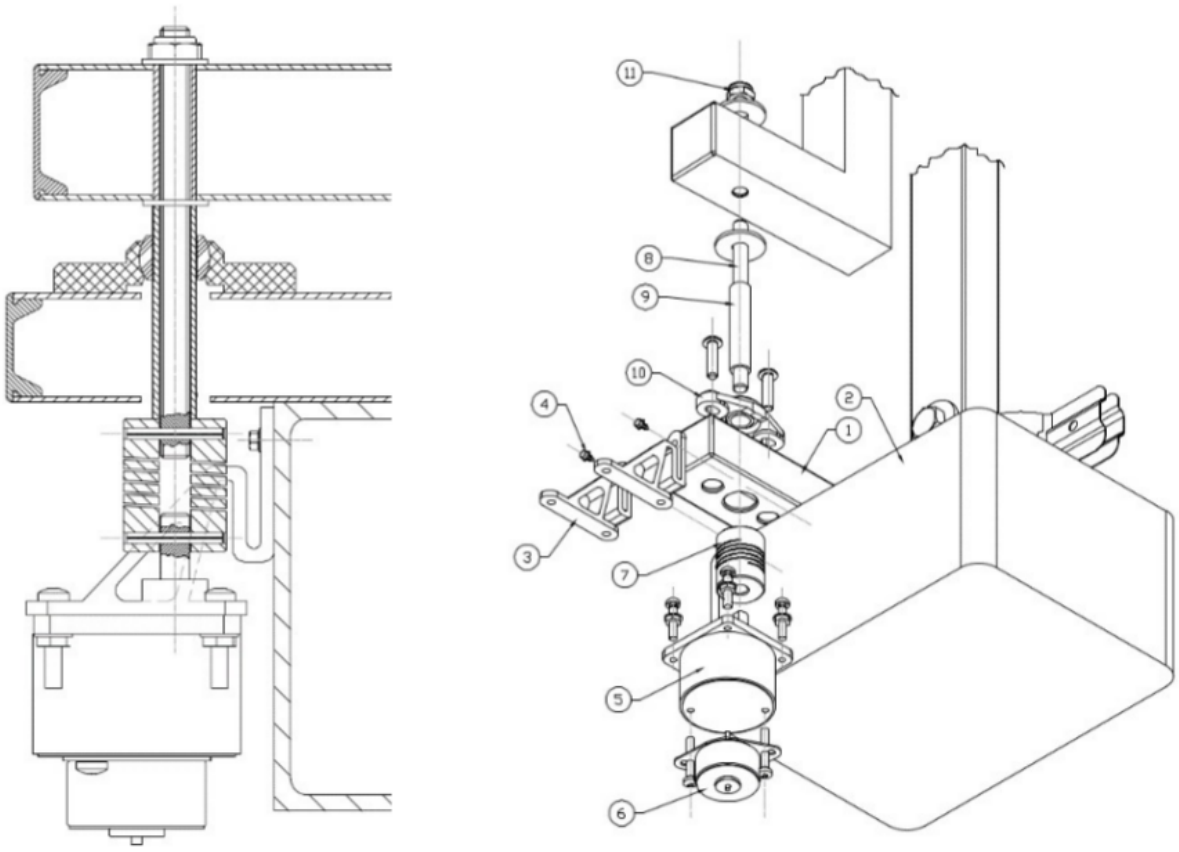

Fig. 22: Figure 3-23 Engine and second reducer mounting representation

In this prototype, engines are mounted directly on the structure. In future, obviously, they will be put inside a waterproof enclosure.

As said above, for the moment the design process is not finished, and many radical changes will be evaluated in order to make the system more accurate and tough. Engines that are good for this version could be overestimated for further upgraded ones.

CHAPTER 5

Annex A - Cinematic Analysis

This annex is intended to study the kinematic motion of the four-bar linkage. The final objective of this section is to find two direct relations to calculate γ and δ depending on θ with a fixed linkage geometry. Some fundamental variables are defined as follows:

H	the frame AD;
l	the two rockers AB e CD;
h	the coupler BC;
γ, δ	the actual angles between the frame and the rockers;
θ	the angle formed by the coupler and the frame, with a positive sign when the antenna points downwards.

The following equations come from simple geometric considerations:

$$\begin{cases} H = l \cdot \cos\gamma + h \cdot \cos\theta + l \cdot \cos\delta \\ l \cdot \sin\delta = l \cdot \sin\gamma + h \cdot \sin\theta \end{cases} \quad (A.1)$$

rearranging the equations, the following can be obtained:

$$\begin{cases} l \cdot (\cos\gamma + \cos\delta) = H - h \cdot \cos\theta \\ l \cdot (\sin\gamma - \sin\delta) = h \cdot \sin\theta \end{cases} \quad (A.2)$$

extracting l and replacing it in the first equation, it results as:

$$h \cdot \sin\theta \frac{(\cos\gamma + \cos\delta)}{(\sin\gamma - \sin\delta)} = H - h \cdot \cos\theta \quad (A.3)$$

using sum to product identities:

$$\cos\alpha + \cos\beta = 2\cos(\tfrac{\alpha+\beta}{2}) \cdot \cos(\tfrac{\alpha-\beta}{2}) \quad (A.4)$$

$$\sin\alpha - \sin\beta = 2\sin(\tfrac{\alpha-\beta}{2}) \cdot \cos(\tfrac{\alpha+\beta}{2}) \quad (A.5)$$

it is possible to write the following:

$$\frac{\cos\gamma + \cos\delta}{\sin\gamma - \sin\delta} = \frac{2\cos(\frac{\gamma+\delta}{2}) \cdot \cos(\frac{\gamma-\delta}{2})}{2\sin(\frac{\gamma-\delta}{2}) \cdot 2\cos(\frac{\gamma+\delta}{2})} = \cot(\tfrac{\gamma-\delta}{2}) \quad (A.6)$$

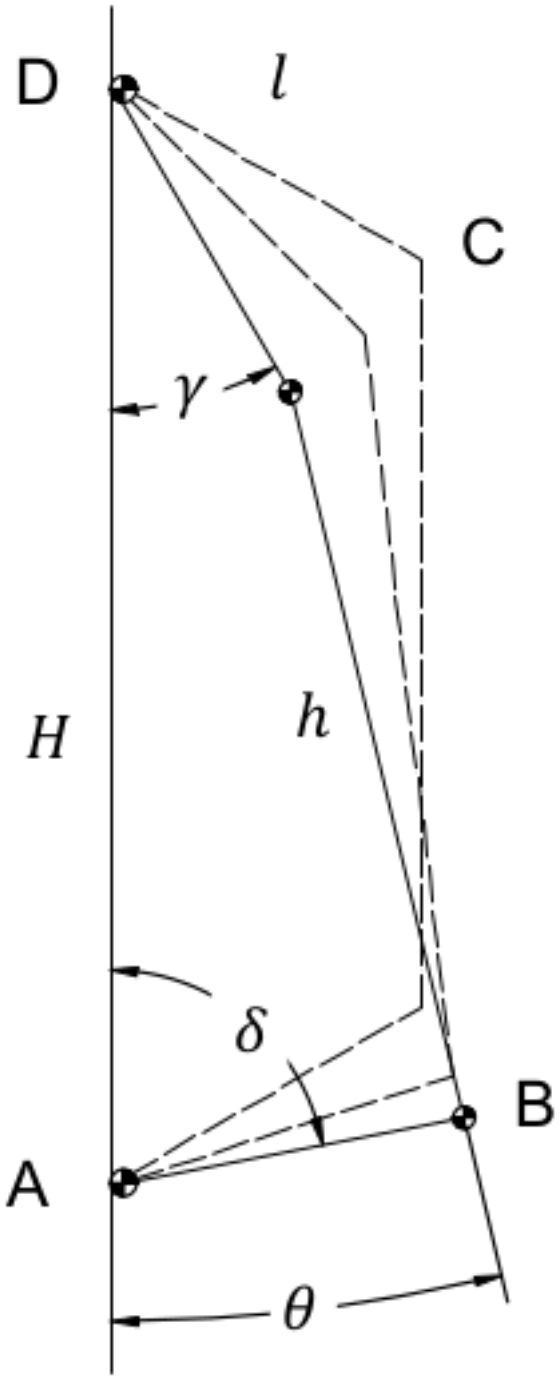

Fig. 1: Figure A-1 The four-bar linkage

and to obtain first key equation:

$$\tan(\tfrac{\gamma-\delta}{2}) = \tfrac{h\cdot\sin\theta}{H-h\cdot\cos\theta} \quad (A.7)$$

Going back to the (A.2), since both the members of the two equations are positive, squaring will not produce a change in the result:

$$\begin{cases} l^2\cdot(\cos\gamma+\cos\delta)^2 = (H-h\cdot\cos\theta)^2 \\ l^2\cdot(\sin\gamma-\sin\delta)^2 = h^2\cdot\sin^2\theta \end{cases} \quad (A.8)$$

expanding the squares:

$$\begin{cases} l^2\cdot(\cos^2\gamma+\cos^2\delta+2\cos\gamma\cdot\cos\delta) = H^2-2H\cdot h\cdot\cos\theta+h^2\cdot\cos^2\theta \\ l^2\cdot(\sin^2\gamma+\sin^2\delta-2\sin\gamma\cdot\sin\delta) = h^2\cdot\sin^2\theta \end{cases} \quad (A.9)$$

and summing them together:

$$l^2\cdot(2+2\cos\gamma\cdot\cos\delta-2\sin\gamma\cdot\sin\delta) = H^2+h^2-2H\cdot h\cdot\cos\theta \quad (A.10)$$

using the difference identity:

$$\cos(\gamma+\delta) = \cos\gamma\cdot\cos\delta-\sin\gamma\cdot\sin\delta \quad (A.11)$$

it's possible to obtain the second key equation:

$$\cos(\gamma+\delta) = \tfrac{H^2+h^2-2H\cdot h\cos\theta}{2\cdot l^2}-1 \quad (A.12)$$

Now, combining the (A.7) with the (A.12), the following system of equations results:

$$\begin{cases} \tan(\tfrac{\gamma-\delta}{2}) = \tfrac{h\cdot\sin\theta}{H-h\cdot\cos\theta} = P \\ \cos(\gamma+\delta) = \tfrac{H^2+h^2-2H\cdot h\cdot\cos\theta}{2\cdot l^2}-1 = Q \end{cases} \quad (A.13)$$

that brings to the final result:

$$\gamma = \tfrac{2\tan^{-1}P+cos^{-1}Q}{2} \quad (A.14)$$

$$\delta = \tfrac{\cos^{-1}Q-2\tan^{-1}P}{2} \quad (A.15)$$

Google Summer of Code

CHAPTER 6

</> GSoC 2018

Name: Marco Musumeci

email: crm.marco@gmail.com

Name of the project: Re-write the Turnantenna code

Project proposal: Google doc

Host organizations: Freifunk, Ninux

6.1 Introduction

This is the first time I can say I seriously coded. In my past experiences I never approached the act of writing code with the final goal of sharing it. Code for yourself is a thing; code for the community, and with the community, is something very different.

I'm not a software developer: I'm a mechanical engineer, and in these three months I've learned a lot of things that I could never learn on my own. I have to say thanks to my mentor and to the Ninux community for the strong support they gave me in this period, and for giving me this possibility. But the time is up, and I'm going to summarise what I achieved during the summer.

6.2 1st period

05/15 - 06/15

During the first month I had to deal with the driver of the engine. The Ninux community developed a first prototype of the Turnantenna, and I started working on it. As the very first step I created a new branch in GitHub called "test", and I continued working on that.

I spent the greater amount of the time writing tests and trying to understand how to improve the pre-existing algorithm. I learned how to use 'unittest', and how to use 'mocks' from zero. It was really challenging.

I wrote a more detailed review of that period in this article.

6.3 2nd period

06/16 - 07/13

In the first week of the second period, I had to complete the previous work on driver tests. After that, I started to work on this documentation. It was a very hard work, and it took all the three weeks remained.

At the same time, I worked on a first version of the States Machine, and learned the basics in order to work with flask and to build the web interface.

The article relative to the work done could be found here

6.4 3rd period

07/14 - 08/14

The last moth was really productive. During the first three weeks I worked on the API definition and the optimization of the States Machine. I learned how to use the 'multiprocessing' module and coded the main process: now it can handle the engine process, the flask RESTful services, and the States Machine.

In the last week I have focused on code refactoring. For this new task I worked on the new dedicated branch "refactor".

Like before, the detailed review of the work is in this article.

6.5 Final conclusions

The initial goal of the project was to write a full working driver and web interface for the Turnantenna. I can say that the 90% of the work was done.

All the code wrote for this project could be found in the dedicated branches in the GitHub project. Links are provided above. There you can find the work done for the Google Summer of Code 2018.

Things done:

- Rewrite the engine driver
- Test the driver
- Write the API
- Test the API
- Create a RESTful web service
- Make things work together

Things to do:

- Make time estimation during the movement of the engine more accurate and correct tests in test_stepmotor.py
- Write the potentiometer "pot_get_position" function
- Implement the system onto the hardware

CHAPTER 7

Indices and tables

- genindex
- modindex
- search